Wind Farm Control under Generator Faults

Ma, Kuichao

DOI (link to publication from Publisher):
10.54337/aau443233806

Publication date:
2021

Document Version
Publisher's PDF, also known as Version of record

WIND FARM CONTROL UNDER GENERATOR FAULTS

BY
KUICHAO MA

DISSERTATION SUBMITTED 2021

AALBORG UNIVERSITY
DENMARK

Wind Farm Control under Generator Faults

Ph.D. Dissertation

Kuichao Ma

Dissertation submitted April, 2021

Dissertation submitted:	April, 2021
PhD supervisor:	Assoc. Prof. Mohsen Soltani Aalborg University
Assistant PhD supervisor:	Prof. Zhe Chen Aalborg University
PhD committee:	Associate Professor Zhenyu Yang (chairman) Aalborg University
	Professor Dr.-Ing. Horst Schulte University of Applied Sciences Berlin
	Associate Professor Christoffer Sloth University of Southern Denmark
PhD Series:	Faculty of Engineering and Science, Aalborg University
Department:	Department of Energy Technology

ISSN (online): 2446-1636
ISBN (online): 978-87-7210-940-4

Published by:
Aalborg University Press
Kroghstræde 3
DK – 9220 Aalborg Ø
Phone: +45 99407140
aauf@forlag.aau.dk
forlag.aau.dk

Printed in Denmark by Rosendahls, 2021

Curriculum Vitae

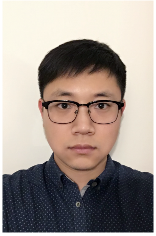

Kuichao Ma

Kuichao Ma received his B. Eng. and M. Sc. degree in electrical engineering from Shengyang University of Technology, China, in 2011 and 2014. He is currently working toward the Ph.D. degree in the Department of Energy Technology, Aalborg University, Aalborg, Denmark. His research interests include generator faults, down-regulation strategy of wind turbine and power optimization of wind farm.

Abstract

Nowadays, the development trend of wind energy has changed from distributed to large-scale wind farms and from onshore to offshore. The special environment of offshore wind energy makes the operation of wind turbines facing more serious challenges than that of onshore wind energy. One of them is the high generator fault rate. The humidity at sea makes the generator failure rate much higher. The maintenance costs of the generator are also high because offshore maintenance usually needs special equipment, such as service vessels. Offshore maintenance is also limited by weather condition, such as wind and wave. At the same time, offshore wind turbines generally have a larger capacity. So the power loss caused by the same downtime is more massive. The wake effect is also a factor that offshore wind farms have to consider.

To solve the problems mentioned above, this thesis studies the control and optimization of offshore wind farms with Doubly-Fed Induction Generator (DFIG)-based wind turbines under generator faults. The objectives include three points: protection of the faulty generator, reduction of the power loss caused by fault, and the optimization of wind farm power. The specific methods are implemented both at the turbine level and the farm level.

The generator faults studied in this thesis include generator cooling system fault and inter-turn short-circuit fault in stator windings. The common feature of these two types of faults is that they are both heat-related. The impact of these two heat-related faults is not very serious at the initial stage. However, ignoring the fault will lead to further deterioration of the fault. Therefore, this thesis adopts derating strategies to protect the faulty wind turbine and avoid excessive power loss compared with shut-down.

The contribution of this thesis is to propose reasonable strategies at the turbine level and the farm level for reducing the impact of generator fault on the wind turbine and wind farm, thereby improving the fault operation capability of wind turbines and reducing the Operation & Maintenance costs of wind farms.

At the turbine level, there are two ways to derate the power of the faulty wind turbine. One is that the faulty wind turbine reduces the faulty phase current through the proposed inter-turn short-circuit fault ride-through strategy. The other is to down-regulate the faulty wind turbine according to the power reference from the wind farm controller. The reference of the faulty wind turbine can not exceed the power limitation calculated by fault model.

At the farm level, particle swarm optimization algorithm is used to optimize the power references of all the wind turbines within the wind farm according to the wind condition, the health condition of the wind turbine and the power demand from the transmission system operator. Furthermore, the down-regulation strategy also has a significant impact on the operating status of the wind turbine and the wind farm. The selection of the specific strategy is based on the health condition of the wind turbine as well. The active power dispatch optimization can reduce the power loss caused by faulty wind turbines and improve the total power while ensuring the safety of the faulty wind turbine.

Resumé

I dag er udviklingen af vindenergi ændret fra distribueret til store vindmølleparker og fra land til offshore. Det specielle miljø med offshore vindenergi gør driften af vindmøller mere udfordrende end vindenergien på land. En af dem er den høje generatorfejlrate. Fugtigheden til søs gør generatorens fejlrate meget højere. Generatorvedligeholdelsesomkostninger er også høje, fordi offshore-vedligeholdelse normalt kræver specielt udstyr såsom serviceskibe. Derudover er offshore vedligeholdelse begrænset af vejrforhold, såsom vind og bølger. Samtidig har havvindmøller generelt større kapacitet. Så strømtabet forårsaget af den samme nedetid er mere massivt. Vækningseffekterne er også en faktor, som havmølleparker skal overveje.

For at tackle ovennævnte spørgsmål studerer denne afhandling styring og optimering af havmølleparker med dobbelt-Fed induktionsgenerator (DFIG) -baserede vindmøller under generatorfejl. Målene inkluderer tre punkter: beskyttelse af den defekte generator, reduktion af effekttabet forårsaget af fejlen og optimering af vindmølleparkens kraft. De specifikke metoder er implementeret både på mølleniveau og på vindmølleparkniveau.

Generatorfejlene undersøgt i denne afhandling inkluderer generators kølesystemfejl og kortslutningsfejl ved drejning i statorviklinger. Det fælles træk ved disse to typer fejl er, at de begge er varme-relaterede. Virkningen af disse to varmerelaterede fejl er ikke særlig alvorlig i den indledende fase. Imidlertid vil ignorering af fejlen føre til yderligere forringelse af fejlen. Derfor vedtager denne afhandling nedsættende strategier for at beskytte den defekte vindmølle og undgå for stort effekttab sammenlignet med nedlukning.

Bidraget fra denne afhandling er at foreslå nye strategier på vindmølle- og vindmølleparkniveau for at reducere virkningen af generatorfejl på vindmøllen og vindmølleparken og derved forbedre funktionsfejl i vindmøllerne og reducere driftsomkostningerne og vedligehold af vindmølleparker.

På vindmølleniveau er der to måder at reducere effekten på den defekte vindmølle. Den ene er, at den defekte vindmølle reducerer den defekte fasestrøm gennem den foreslåede gennemløbsstrategi for kortslutningsfejl. Det andet er at nedregulere den defekte vindmølle i henhold til kraftreferencen fra vindmølleparkens controller. Referencekravet til den defekte vindmølle kan ikke overstige den effektgrænse, der er beregnet af fejlmodellen.

På vindmølleparkniveau bruges partikel-sværmoptimeringsalgoritme til at optimere effektreferencer for alle vindmøller i vindmølleparken i henhold til vindtilstanden, vindmøllens sikkerhedstilstand og effektbehovet fra transmissionssystemoperatøren. Derudover har nedreguleringsstrategien også en væsentlig indflydelse på driftsstatus for vindmøllen og vindmølleparken. Valget af den specifikke strategi er også baseret på vindmøllens sikkerhedstilstand. Optimering af aktiv kraftoverførsel kan reducere effekttabet forårsaget af defekte vindmøller og forbedre den samlede effekt, mens det sikrer sikkerheden for den defekte vindmølle.

Contents

Preface

This thesis is submitted as a collection of papers in fulfilment of the requirements for the degree of Doctor of Philosophy at the Department of Energy Technology, Aalborg University, Denmark. The work has been carried out at the Department of Energy Technology, Aalborg University Campus Esbjerg, in the period from January 2017 to June 2020 under the supervision of Associate Professor Mohsen Soltani and Professor Zhe Chen. During this research period, I have been a visiting scholar at National Renewable Energy Laboratory, USA, from December 2018 to February 2019 under the supervision of Senior Engineer Katherine Dykes.

I would like to express my deep and sincere gratitude to my supervisor Associate Professor Mohsen Soltani for offering me the opportunity to pursue my Ph.D. study and giving me so much guidance and help during the study period. His rich knowledge and unique insights deeply inspired me. It is a great honour to work and study under his guidance.

I would like to sincerely acknowledge my co-supervisor Professor Zhe Chen and Associate Professor Amin Hajizadeh for their thoughtful comments and recommendations on the papers and the research. Then, I would like to thank Senior Engineer Katherine Dykes for her invitation to NREL and thank Senior Engineer Derek Berry and other friends for their help during my stay in the USA.

I appreciate my friend Jiangsheng Zhu recommended me to pursue a Ph.D. degree in Denmark and offered me so much help and many constructive suggestions. I would also like to thank all my colleagues and friends who helped me in different ways. It is a very pleasant experience for me to know and work with them.

Last but not least, I am extremely grateful to my parents for their care, love and support. I will also express my thanks to my wife for her love, understanding and continuing support.

Kuichao Ma
Aalborg University, April 2021

Part I

Extended Summary

1 Introduction

1.1 Background

Wind energy is currently one of the most widely used renewable energy sources. Fig. 1 shows the global wind energy installation. As of the end of 2019, the cumulative installed capacity of wind power reached 651 GW [33].

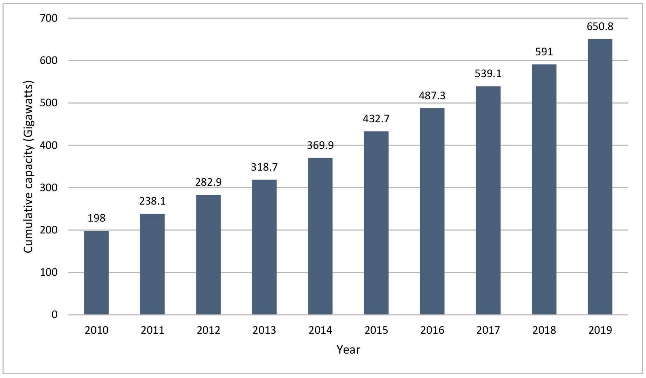

Fig. 1: Global wind power cumulative power capacity (Data: GWEC).

The total installed capacity of wind turbines can meet more than 6% of the world's electricity demand [3]. In 2019, the capacity of wind power in Europe was 205 GW. Wind energy accounted for 15% of the electricity consumed by EU-28 countries. In Denmark, wind energy accounted for up to 48% of the electricity demand [57].

Recently, offshore wind farms have attracted more and more attention due to many advantages such as higher and more stable wind speed than onshore wind farms [1]. Offshore wind energy provides a significant contribution to global wind energy installations [2]. However, the harsh environment of offshore wind farms leads to many difficulties to the development. First of all, compared with onshore wind farms, the humidity of offshore wind farms is much higher. High humidity will increase the failure rate of the components of wind turbines, especially generators and converters [11, 52]. The maintenance of offshore wind turbines requires special types of equipment and vessels. The Operation & Maintenance (O&M) costs are much higher, accounting for 20-40% of Cost of Energy (COE) [42]. Furthermore, the maintenance of offshore wind farms is also affected by weather condition, such as wind and wave. The sudden shut-down may lead to more extended downtime. During the same downtime, the power loss of offshore wind turbines is greater than that of onshore wind turbines due to the large capacity of offshore wind turbines. Therefore, the impact of many faults on offshore wind farms is more significant than that of onshore wind farms. It is essential to deal with the faults reasonably and effectively during the operation of offshore wind farms.

As one of the most critical components of the wind turbine, a generator converts mechanical energy into electrical energy. It can be seen from some relevant research that the failure rate of generators is very high, and the downtime caused by generator failure is quite long [49]. Therefore, this thesis studies the control and optimization of offshore wind farms with the Doubly-Fed Induction Generator (DFIG) based wind turbines under generator faults. Among many generator faults, generator cooling system fault and Inter-Turn Short-Circuit (ITSC) fault in stator winding are studied. Both of these two faults are heat-related. They have some same features in common:

- At the early stage of the fault, the impact of the fault is not great. But the long-term operation without considering these faults will lead to further damage to the generator.
- The direct reason of generator failure caused by the fault is the premature ageing of winding insulation. As a rule of thumb, the insulation lifetime is reduced by half for each 10°C; that motor temperature exceeds its rated insulation temperature [56]. The main heat source of the stator is the current in the winding. The reduction of the current can decrease the impact of the fault.

For this sort of fault, the directly shut-down will cause unnecessary power loss. However, ignoring faults will lead to further damage of the generator.

1.2 Research Objective

The objective of this thesis is to minimize the impact of the fault on the wind farm power output under the premise of protecting the faulty generator by turbine level control and farm level optimization. In theory, the combination of turbine level and farm level can integrate different levels of regulation and improve the overall controllability of the farm. In practice, these methods can improve the ability of wind farms to operate safely under faults, provide more flexibility to the maintenance strategy, and enhance the competitiveness of wind power in the field of renewable energy.

1.3 Research Hypothesis

According to the previous description, derating has the potential to protect the generator under heat-related faults. But derating also has a negative influence on the wind turbine and the wind farm on power production.

To make the wind farm operate safely and reliably under generator faults, the analysis of the specific fault is necessary. The reasonable treatments should be adopted to protect the faulty generator. The methods can be carried out at the turbine level or at the farm level. Since the power limitation of the faulty turbine will directly affect the aerodynamic interactions among wind turbines, the fault treatment must be considered in the wind farm power regulation. At the same time, the wake effect is also a factor that wind farms can not ignore. Thus, in relation to protecting the faulty generator and operating wind farms reliably, the research hypotheses is as follows:

- It is possible to protect the generator through derating under heat-related generator fault while minimizing the power loss caused by wake effects and generator protection through down-regulation and active power dispatch optimization.

1.4 Outline of the Papers

The thesis consists of an extended summary and the published papers. The extended summary describes the research background, content and the summary of the papers.

The following are the chronology and the description of the papers.

Paper A This paper mainly introduces the basic ideas when generator faults occur in the wind farm. Both shut-down and continuing operating the faulty wind turbine as normal are not appropriate without considering the severity of the fault. Therefore, this paper divides the generator faults into three levels. Based on the severity of the fault, three different treatments are adopted: continuing operating the faulty wind turbine as normal for the faults with low severity; down-regulation for the faults with medium severity; shut-down for severe faults. An active power reference distribution based on proportional dispatch strategy with consideration of wake effects is proposed to track the power demand from Transmission System Operator (TSO). The priority of generator fault protection is higher than power demand tracking.

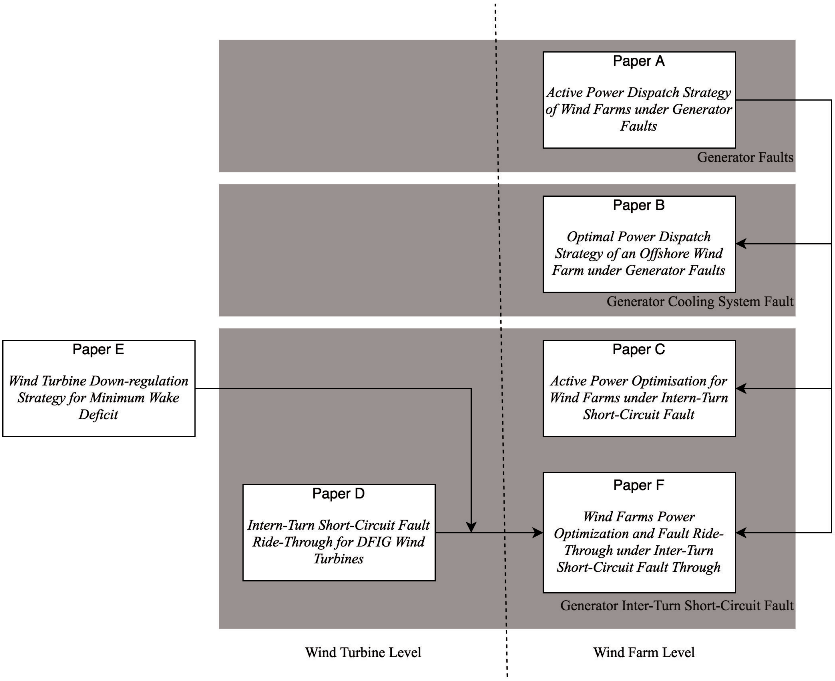

Fig. 2: Chronology of papers

Paper B The fault studied in this paper is the generator cooling system fault at the early stage. The simplified thermal model shows that the thermal resistance increases when the fault occurs. As the heat source, the generator current needs to be reduced to prevent the temperature rise from exceeding the normal value. So at the turbine level, the faulty wind turbine is down-regulated. The specific power limitation that the faulty turbine should be down-regulated to is obtained from the temperature rise curve. The temperature rise curve depends on the changed thermal resistance. At the wind farm level, Particle Swarm Optimization (PSO) algorithm is used to meet the power demand from TSO with considering wake effects and power limitation of the faulty wind turbine. The active power references of all the wind turbines are the optimization variables. The results show that the proposed method can effectively protect the generator when the generator cooling system fault occurs, and reduce the impact of the down-regulation on the power output of the wind farm.

Paper C This paper studies the ITSC fault in the stator winding of DFIG. The power limitation corresponding to the different fault level is obtained based on the ITSC fault model. At the turbine level, the power output of the faulty wind turbine will be limited to this power limitation to prevent the faulty phase current from exceeding the rated value. At the farm level, similar to Paper B, the active power references are optimized by PSO. The limitation of the faulty wind turbine is regarded as one of the optimization constraints. The results show that the proposed method can down-regulate the faulty wind turbine to an appropriate power limitation with a known fault level. The power optimization of the wind farm can reduce the power loss caused by the faulty wind turbine.

Paper D This paper studies the ITSC fault in the stator winding of DFIG as well. Different from Paper C, the ITSC fault ride-through strategy at the turbine level adopted in Paper D does not require the specific fault level. The advantage of the ITSC fault-ride through strategy is that it can avoid the problem caused by the error of the fault level estimation. When the model-based closed-loop state observer detects an ITSC fault, the strategy decides whether it should down-regulate the wind turbine according to faulty phase current. The specific down-regulation method depends on the operation region. The difference between the faulty phase current and the rated value with the proportion-integration operation is superimposed to the original generator torque reference or the pitch angle reference. The results show that this strategy can effectively down-regulate the faulty wind turbine within the safe power range without knowing the fault level.

Paper E To reduce the wake effect of the upstream wind turbines and improve the power generation capacity of wind farms, this paper proposes a Minimum C_t (Min-C_t) down-regulation strategy. After receiving the power reference, the values of C_t of all the operating points that meet this power reference are calculated. Then, the operating point with the minimum C_t value is set as the control objective. The generator torque and the pitch angle of the wind turbine are adjusted to the corresponding reference values. The results show that Min-C_t can reduce the wake effect of the upstream wind turbine and increase the wind speed of the downstream wind turbine. The wind farms applying this strategy can improve the power generation capacity to further reduce the power loss caused by the faulty wind turbine.

Paper F The proposed stator ITSC fault-ride through strategy and Min-C_t strategy are adopted at the turbine level in Paper F. Since Min-C_t strategy can reduce the power limitation under ITSC fault in the stator winding, Min-C_t strategy is used for the healthy wind turbines to improve the power of wind farms while Maximum-ω (Max-ω) strategy is applied for the faulty wind turbines to avoid more power loss. ITSC fault ride-through strategy is used to protect the faulty wind turbine. Due to the command of the down-regulation is not through the power reference, the power limitation does not need to be considered in the process of power optimization of wind farms. The results show that the switching of the down-regulation strategy can improve the power output of wind farms and avoid the decrease of the power limitation of the faulty wind turbine.

2 Wind Farm Model and Fault Models

A wind farm is also called wind park or wind power plant, which refers to the power plant that uses wind energy to generate electricity. The number of wind turbines in a wind farm can range from as few as two or three, and as many as several thousand. According to the location, wind farms can be divided into onshore wind farms and offshore wind farms. For grid-connected wind farms, power needs to be issued according to the power demand from TSO during operation. The total power output of a wind farm is composed of the power generated by all the wind turbines. Fig. 3 shows a typical electrical topology of a wind farm.

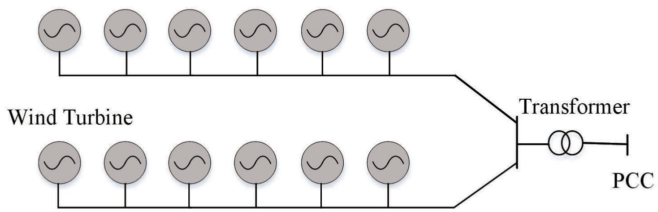

Fig. 3: Electrical topology of wind farm.

From the perspective of the power output of wind farms, the wind farm can be regarded as composed of three factors: wind turbines, aerodynamic interactions among wind turbines and the layout of wind turbines. This chapter describes these three factors separately and the models of the studied faults.

2.1 DFIG Wind Turbine

DFIG wind turbine is a variable speed constant frequency wind turbine with DFIG as the generator, and it is one of the most widely used models. The structure of a DFIG wind turbine is shown in Fig. 4.

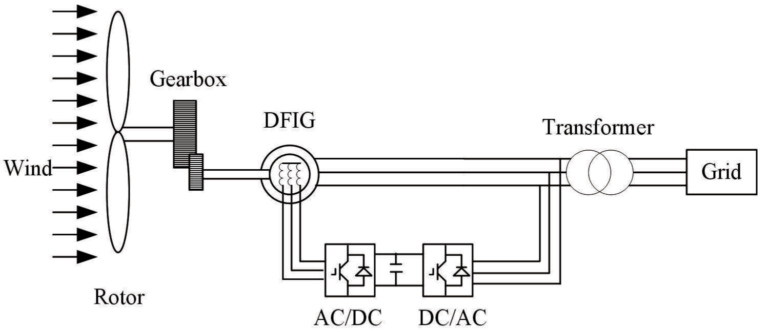

Fig. 4: Structure of DFIG wind turbines.

In the electrical structure, the stator windings of the DFIG wind turbine are directly connected to the grid, and the rotor windings are indirectly connected to the grid by a back to back converter. In the mechanical structure, the generator shaft is connected to the main shaft using a gearbox. DFIG wind turbines have many advantages [40, 43]:

- The active power and reactive power can be controlled separately.
- The capacity of the converter is only about 30% of that of the wind turbine.
- The wide speed range is conductive to extract the optimal power.

In this thesis, the modified NREL 5 MW wind turbine model in SimWindFarm Simulink toolbox [23] is adopted. For the study that does not involve the dynamic characteristics of the generator and only considers the power of the wind farm, the static model of the wind turbine is sufficient. Fig. 5 shows the wind turbine static model, where P_{r} is the power reference of the WT; v is the wind speed; β is the pitch angle; λ is the tip speed ratio; C_{p} is the power coefficient; ρ is the air density; R is the radius of the rotor of the turbine; P is the power output.

The inputs of this model are the power reference, P_{r}, and the wind speed, v. The outputs are the power output, P, and the thrust coefficient, C_{t}. The controller of the wind turbine sends the reference of pitch angle, β, and the reference of tip speed ratio, λ, to the pitch system and the generator system according to control strategy. The power coefficient, C_{p}, and C_{t} depend on β, λ. The surfaces of C_{p} and C_{t} in Fig. 5 show their relationships. The power output of the wind turbine is given by

$$P = \frac{1}{2}\rho\pi R^2 v^3 C_{\mathrm{p}}\eta, \tag{1}$$

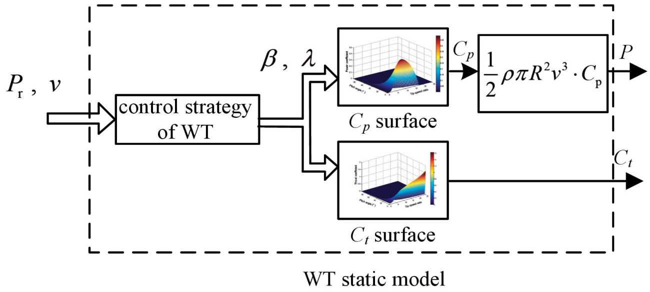

Fig. 5: Wind turbine static model.

where ρ is the air density; R is the radius of the turbine rotor; η is the conversion efficiency. Fig. 6 shows the power curve of this wind turbine model.

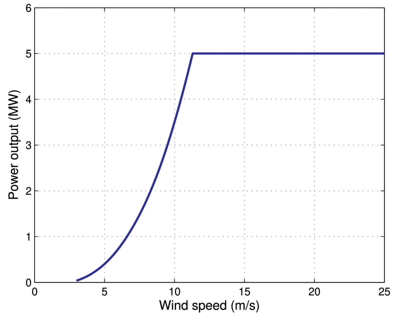

Fig. 6: Power curve of the adopted wind turbine model.

For the method of using derating to protect the faulty generator, the impact of the down-regulation strategy on wind turbines and wind farms cannot be ignored. Fig. 7 shows the surfaces of pitch angle, rotor speed, C_p and C_t in Max-ω strategy.

v and P_r are the x-axis and y-axis respectively in these four sub-figures. It can be seen from the surfaces of pitch angle and rotor speed that the pitch angle increases and the rotor speed goes up to the rated value when the WT is derated.

In the derating mode, the power reference of the wind turbine is lower than the value on the designed power curve. The wind turbine is down-regulated by its controller according to the down-regulation strategy.

Max-ω strategy is the most widely used down-regulation strategy. The analysis in Paper F shows that the power limitation under Max-ω strategy is higher than that under Min-C_t strategy when the stator ITSC fault occurs. Min-C_t strategy proposed in Paper E can minimize the value of C_t when the

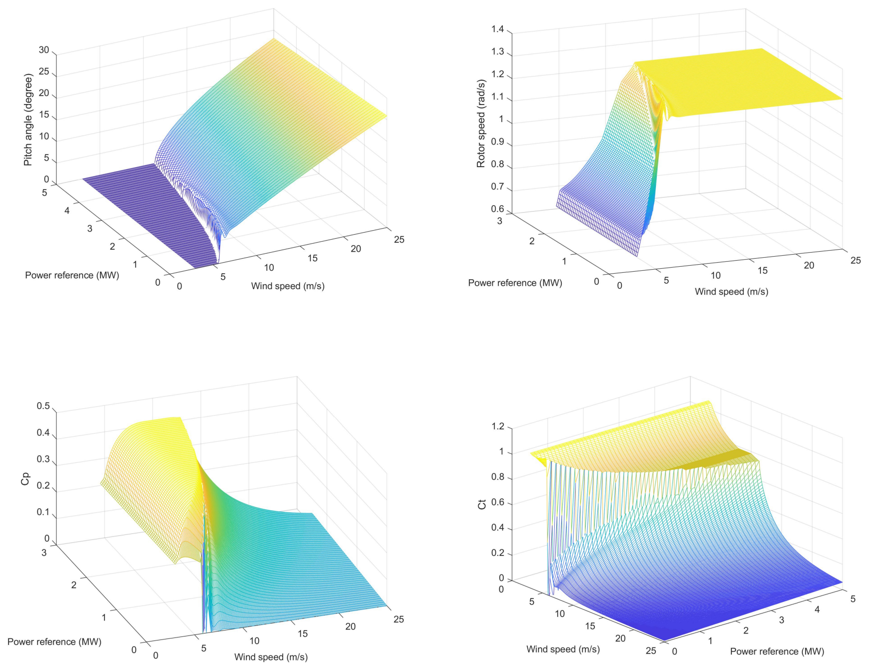

Fig. 7: Surfaces of pitch angle, rotor speed, C_p and C_t in Max-ω down-regulation strategy.

wind turbine is down-regulated and have the potential to improve the power of wind farms.

2.2 Wake Effect

The wake effect is one of the factors that cannot be ignored in wind farm research. When the wind turbine extracts energy from the wind, it will generate a wake to the free wind behind the turbine. The main effects of wake are the decrease in wind speed and the increase of turbulence. When the downstream wind turbine is in the wake of the upstream wind turbine, the wake will cause a decrease in power and an increase in dynamic loads of the downstream wind turbine [20]. Therefore, no matter from the perspective of the power or loads, the study of the wake is essential in wind farms.

The control and optimization of wind farms require wake models. In recent decades, there are many related studies on wake models [22, 45]. The CFD simulation is accurate, but due to the high computational cost, it is difficult to use in control. Although the analytical model is less accurate, its computational cost is quite low. Therefore, analytical models are quite suitable for the optimization of wind farm layout and the control of wind farm with flat terrain [45]. Since this thesis mainly focuses on the control and optimization of wind turbines and wind farms under fault conditions, the widely used Jensen model is adopted. The scheme of Jensen wake model is shown in Fig. 8.

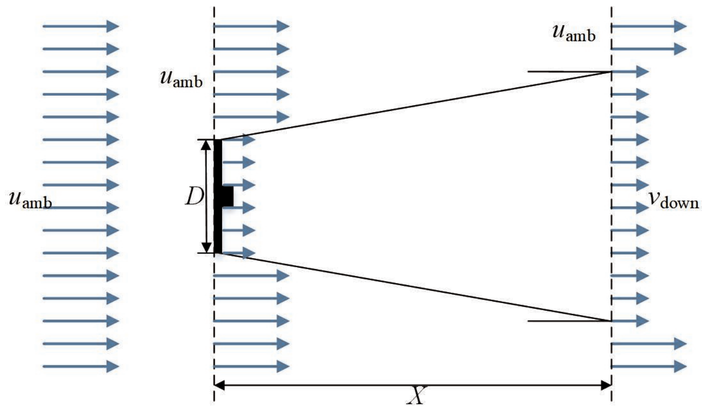

Fig. 8: Scheme of Jensen wake model.

Jensen wake model can be expressed by

$$\frac{v_{down}}{u_{amb}} = \frac{1-\sqrt{1-C_t}}{(1+2\alpha X/D)^2}, \tag{2}$$

where v_{down} is the wind speed of the downstream WT; u_{amb} is the ambient free wind speed; X is the distance between the upstream and the downstream wind turbines; D is the diameter of the rotor of the turbine; α is the decay coefficient, which choosing 0.05 for offshore wind farms [27]; C_t is the thrust coefficient of the upstream WT.

The multiple wakes can be calculated by quadratic summation method and expressed by

$$(1-\frac{v_j}{u})^2 = \sum_{i=1}^{n}(1-\frac{v_{ij}}{u})^2, \tag{3}$$

where v_j is the wind speed of the j^{th} wind turbine; n is the number of wakes that the j^{th} wind turbine is in; v_{ij} is the wind speed of the j^{th} wind turbine under the impact of the wake of the i^{th} wind turbine.

2.3 Wind Farm Layout

The layout of wind turbines is one of the most important attributes of wind farms. It can directly affect the power generation capacity of wind farms. Therefore, wind farm layout is also a factor that must be determined in wind farm power research. It can be seen from the wake model that the larger the wind turbine spacing, the smaller the wake effect. However, the excessively large spacing will result in high investment costs. Typically, the wind turbine spacing of offshore wind farms is 5 to 15 times the diameter of the rotor of the wind turbine [48]. To more clearly see the impact of wake and the effect of the proposed method, the wind direction that makes all wind turbines under full wake condition is adopted. First, a simulation is made to determine the reasonable quantity of wind turbines. All wind turbines operate under the conventional control strategy. The inflow wind speed is 12 m/s. The wind turbine spacing is 6.5 times the diameter of the rotor. Five wind turbines are arranged in a straight line. Fig. 9 shows the wind speed distribution of all wind turbines.

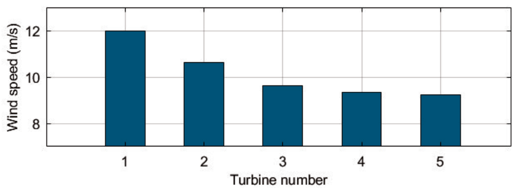

Fig. 9: Wind speed distribution of 5 wind turbines.

It can be seen that due to the wake effect, the wind speed of the second wind turbine is significantly reduced. But this effect will gradually be smaller in later wind turbines. The wind speed difference between the fourth and the fifth wind turbines is already very small.

Therefore, this thesis adopts 5 wind turbines in a straight-line arrangement with 6.5 times diameter spacing under full wake condition. The wind farm layout is shown in Fig. 10.

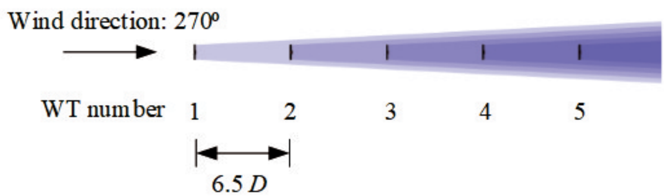

Fig. 10: Wind farm layout.

2.4 Simplified Thermal Model of Stator Winding

The fault of the generator cooling system has a direct impact on the temperature rise of the generator. Excessive temperature will greatly reduce the life of the winding insulation. When the cooling capacity of the cooling system drops at the early stage of some faults, shutting down the faulty wind turbine directly will cause unnecessary power loss. To avoid excessive temperature under fault conditions, reducing the generator heat is another solution. The electro-thermal model of the generator is very complicated, so this thesis only analyses the temperature rise of the stator winding under the cooling system fault. According to [6, 47], the simplified thermal model of the stator winding is shown in Fig. 11, where P_{loss} is the power loss of the stator winding; R_{th} is the thermal resistance; θ_{amb} is the ambient temperature; C_{th} is the thermal capacity; θ is the temperature of the stator winding.

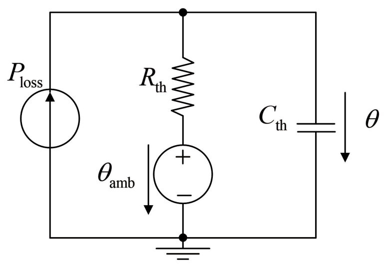

Fig. 11: Simplified thermal model of stator winding.

Through the steady-state analysis of this simplified thermal model, we can get the expression of θ as follows

$$\theta = P_{\text{loss}} R_{\text{th}} + \theta_{\text{amb}}. \tag{4}$$

Assuming θ_{amb} is constant, the temperature rise depends on P_{loss} and R_{th}. According to the analysis and data mentioned in [47], when the circulation of the heat dissipation medium in the cooling system slows down, but the cooling medium does not change, R_{th} increases while C_{th} remains the same. Therefore, appropriately reducing P_{loss} by down-regulation of the generator can ensure that the temperature rise is within a reasonable range.

2.5 DFIG Model with Inter-Turn Short-Circuit

DFIG model under healthy condition The fault type studied in this thesis is the ITSC fault of the single-phase stator winding of DFIG. To clearly show the influence of the fault on the mathematical model, the mathematical model of DFIG in the a-b-c coordinates under healthy condition is described here. The mathematical model of DFIG can be expressed by voltage equation, magnetic flux equation, torque equation and motion equation [32].

Voltage equation:

$$\boldsymbol{u} = \boldsymbol{R}\boldsymbol{i} + \frac{d}{d\mathrm{t}}\boldsymbol{\psi}, \tag{5}$$

where the italic bold letters donate the vectors and matrices; $\boldsymbol{u}$ is the voltage vector; $\boldsymbol{R}$ is the resistance matrix; $\boldsymbol{i}$ is the current vector; $\boldsymbol{\psi}$ is the magnetic flux vector. The details are given by

$$\begin{cases} \boldsymbol{u} = [u_{\mathrm{A}}, u_{\mathrm{B}}, u_{\mathrm{C}}, u_{\mathrm{a}}, u_{\mathrm{b}}, u_{\mathrm{c}}]^T \\ \boldsymbol{i} = [i_{\mathrm{A}}, i_{\mathrm{B}}, i_{\mathrm{C}}, i_{\mathrm{a}}, i_{\mathrm{b}}, i_{\mathrm{c}}]^T \\ \boldsymbol{\psi} = [\psi_{\mathrm{A}}, \psi_{\mathrm{B}}, \psi_{\mathrm{C}}, \psi_{\mathrm{a}}, \psi_{\mathrm{b}}, \psi_{\mathrm{c}}]^T \\ \boldsymbol{R} = \begin{bmatrix} R_{\mathrm{A}} & 0 & 0 & 0 & 0 & 0 \\ 0 & R_{\mathrm{B}} & 0 & 0 & 0 & 0 \\ 0 & 0 & R_{\mathrm{C}} & 0 & 0 & 0 \\ 0 & 0 & 0 & R_{\mathrm{a}} & 0 & 0 \\ 0 & 0 & 0 & 0 & R_{\mathrm{b}} & 0 \\ 0 & 0 & 0 & 0 & 0 & R_{\mathrm{c}} \end{bmatrix} \end{cases}, \tag{6}$$

where the subscripts A, B and C denote the phase A, B and C in stator; the subscripts a, b and c denote the phase a, b and c in rotor; u_{A}, u_{B}, u_{C}, u_{a}, u_{b} and u_{c} are the voltages of each phase; i_{A}, i_{B}, i_{C}, i_{a}, i_{b} and i_{c} are the currents of each phase; ψ_{A}, ψ_{B}, ψ_{C}, ψ_{a}, ψ_{b} and ψ_{c} are the magnetic fluxes of each phase; R_{A}, R_{B}, R_{C}, R_{a}, R_{b} and R_{c} are the resistances of each phase.

Magnetic flux equation:

$$\boldsymbol{\psi} = \boldsymbol{L}\boldsymbol{i}, \tag{7}$$

where $\boldsymbol{L}$ is the inductance matrix composed of all the self and mutual inductances:

$$\boldsymbol{L} = \begin{bmatrix} L_{\mathrm{AA}} & L_{\mathrm{AB}} & L_{\mathrm{AC}} & L_{\mathrm{Aa}} & L_{\mathrm{Ab}} & L_{\mathrm{Ac}} \\ L_{\mathrm{BA}} & L_{\mathrm{BB}} & L_{\mathrm{BC}} & L_{\mathrm{Ba}} & L_{\mathrm{Bb}} & L_{\mathrm{Bc}} \\ L_{\mathrm{CA}} & L_{\mathrm{CB}} & L_{\mathrm{CC}} & L_{\mathrm{Ca}} & L_{\mathrm{Cb}} & L_{\mathrm{Cc}} \\ L_{\mathrm{aA}} & L_{\mathrm{aB}} & L_{\mathrm{aC}} & L_{\mathrm{aa}} & L_{\mathrm{ab}} & L_{\mathrm{ac}} \\ L_{\mathrm{bA}} & L_{\mathrm{bB}} & L_{\mathrm{bC}} & L_{\mathrm{ba}} & L_{\mathrm{bb}} & L_{\mathrm{bc}} \\ L_{\mathrm{cA}} & L_{\mathrm{cB}} & L_{\mathrm{cC}} & L_{\mathrm{ca}} & L_{\mathrm{cb}} & L_{\mathrm{cc}} \end{bmatrix}. \tag{8}$$

The self inductances are as follows:

$$\begin{cases} L_{\mathrm{AA}} = L_{\mathrm{BB}} = L_{\mathrm{CC}} = L_{\mathrm{m}} + L_{\mathrm{œs}} \\ L_{\mathrm{aa}} = L_{\mathrm{bb}} = L_{\mathrm{cc}} = L_{\mathrm{m}} + L_{\mathrm{œr}} \end{cases}, \tag{9}$$

where L_{m} is the mutual inductance of the stator and the rotor; $L_{\mathrm{œs}}$ and $L_{\mathrm{œr}}$ are the leakage inductances of the stator and the rotor.

The mutual inductances are as follows:

$$\begin{cases} L_{\mathrm{AB}} = L_{\mathrm{BC}} = L_{\mathrm{CA}} = L_{\mathrm{BA}} = L_{\mathrm{CB}} = L_{\mathrm{AC}} = -\frac{1}{2}L_{\mathrm{m}} \\ L_{\mathrm{ab}} = L_{\mathrm{bc}} = L_{\mathrm{ca}} = L_{\mathrm{ba}} = L_{\mathrm{cb}} = L_{\mathrm{ac}} = -\frac{1}{2}L_{\mathrm{m}} \\ L_{\mathrm{Aa}} = L_{\mathrm{aA}} = L_{\mathrm{Bb}} = L_{\mathrm{bB}} = L_{\mathrm{Cc}} = L_{\mathrm{cC}} = L_{\mathrm{m}}\cos\theta \\ L_{\mathrm{Ab}} = L_{\mathrm{bA}} = L_{\mathrm{Bc}} = L_{\mathrm{cB}} = L_{\mathrm{Ca}} = L_{\mathrm{aC}} = L_{\mathrm{m}}\cos(\theta + \frac{2}{3}\pi) \\ L_{\mathrm{Ac}} = L_{\mathrm{cA}} = L_{\mathrm{Ba}} = L_{\mathrm{aB}} = L_{\mathrm{Cb}} = L_{\mathrm{bC}} = L_{\mathrm{m}}\cos(\theta - \frac{2}{3}\pi) \end{cases}, \tag{10}$$

where θ is the electrical angle between the stator and the rotor.

Torque equation:

$$\begin{aligned} T_{\mathrm{e}} = &- n_{\mathrm{p}}L_{\mathrm{m}}[(i_{\mathrm{A}}i_{\mathrm{a}} + i_{\mathrm{B}}i_{\mathrm{b}} + i_{\mathrm{C}}i_{\mathrm{c}})\sin\theta \\ &+ (i_{\mathrm{A}}i_{\mathrm{b}} + i_{\mathrm{B}}i_{\mathrm{c}} + i_{\mathrm{C}}i_{\mathrm{a}})\sin(\theta + \frac{2}{3}\pi) \\ &+ (i_{\mathrm{A}}i_{\mathrm{c}} + i_{\mathrm{B}}i_{\mathrm{a}} + i_{\mathrm{C}}i_{\mathrm{b}})\sin(\theta - \frac{2}{3}\pi)] \end{aligned}, \tag{11}$$

where T_{e} is the electromagnetic torque; n_{p} is the number of pole pairs.

Motion equation:

$$\frac{J}{n_{\mathrm{p}}}\frac{d\omega_{\mathrm{r}}}{dt} = T_{\mathrm{m}} - T_{\mathrm{e}}, \tag{12}$$

where J is the total moment of inertia; ω_{r} is the mechanical rotor speed; T_{m} is the mechanical torque.

Definition of ITSC fault The stator windings of DFIG are generally composed of three-phase symmetrical distributed windings with a difference of 120°. in space. The windings designed in this way can make the air gap magnetic field generated by the three-phase symmetrical current meet the requirements of basic sinusoidal distribution.

To represent the relationship the electrical and magnetic relationships of DFIG under stator ITSC fault, this thesis regards the shorted turns as a new phase. This strategy has been adopted in some research works [35, 55]. In this way, the original three-phase stator winding of DFIG becomes four-phase, as shown in Fig. 12.

In Fig. 12, A, B, and C represent the three-phase windings of the stator. Assuming that the ITSC fault occurs in Phase A, the fault divides Phase A into two parts: un-shorted turns A1 and shorted turns A2. R_{f} is the insulation break resistance, and i_{f} is the short circuit current. To facilitate the analysis of the model, the following assumptions are made:

- Magnetic saturation and spatial harmonics are ignored, and the self-inductance and mutual inductance of each winding are fixed values.

- Each stator phase has the same number of turns.

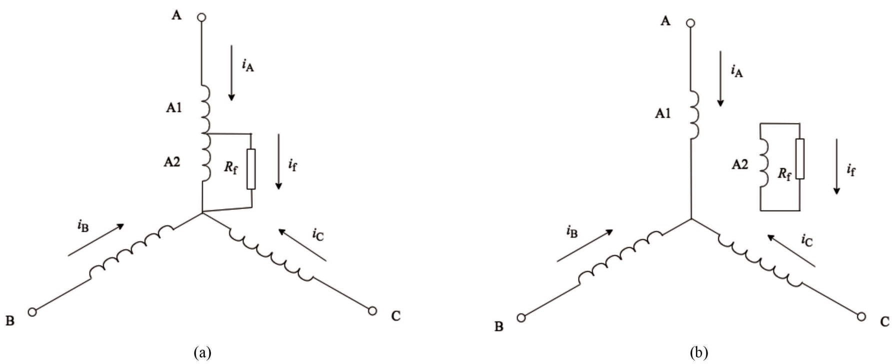

Fig. 12: Stator structure of DFIG with ITSC fault in Phase A.

- The three-phase windings are symmetrical in space, and the magnetomotive force is sinusoidally distributed along the air gap.
- The insulation break resistance R_f is negligible.

Since it has been assumed that the ITSC fault occurs in Phase A, the fault can be defined by the fault level μ. The fault level μ is used to represent the severity of ITSC fault and expressed as the percentage of the shorted turns in the original turns:

$$\mu = \frac{N_f}{N_s} \times 100\%, \tag{13}$$

where $N_f$is the number of the shorted turns; N_s is the total number of the original turns in the stator winding; μ is a percentage from 0% to 100%. $\mu = 0\%$ means the winding is healthy.

DFIG model with ITSC fault From Fig. 12 we can see that the ITSC fault changes the DFIG stator from the original three-phase to four-phase. Because the shorted turns are regarded as a new phase, the self-inductance, mutual inductance and other parameters of the faulty phase will change accordingly. By adding these changes to the DFIG model under healthy condition, we can get the DFIG model with ITSC fault as follows:

Voltage equation: The vectors and matrices in Eq. (5) are

$$\begin{cases} \boldsymbol{u} = [u_{\mathrm{A}}, 0, u_{\mathrm{B}}, u_{\mathrm{C}}, u_{\mathrm{a}}, u_{\mathrm{b}}, u_{\mathrm{c}}]^T \\ \boldsymbol{i} = [i_{\mathrm{A}}, i_{\mathrm{A}} - i_{\mathrm{f}}, i_{\mathrm{B}}, i_{\mathrm{C}}, i_{\mathrm{a}}, i_{\mathrm{b}}, i_{\mathrm{c}}]^T \\ \boldsymbol{\psi} = [\psi_{\mathrm{A1}}, \psi_{\mathrm{A2}}, \psi_{\mathrm{B}}, \psi_{\mathrm{C}}, \psi_{\mathrm{a}}, \psi_{\mathrm{b}}, \psi_{\mathrm{c}}]^T \\ \boldsymbol{R} = \begin{bmatrix} R_{\mathrm{A1}} & 0 & 0 & 0 & 0 & 0 & 0 \\ 0 & R_{\mathrm{A2}} & 0 & 0 & 0 & 0 & 0 \\ 0 & 0 & R_{\mathrm{B}} & 0 & 0 & 0 & 0 \\ 0 & 0 & 0 & R_{\mathrm{C}} & 0 & 0 & 0 \\ 0 & 0 & 0 & 0 & R_{\mathrm{a}} & 0 & 0 \\ 0 & 0 & 0 & 0 & 0 & R_{\mathrm{b}} & 0 \\ 0 & 0 & 0 & 0 & 0 & 0 & R_{\mathrm{c}} \end{bmatrix} \end{cases}, \tag{14}$$

where the subscripts A1, A2 denote the un-shorted and the shorted phases, respectively; ψ_{A1} and ψ_{A2} are the magnetic fluxes of Phase A1 and Phase A2; R_{A1} and R_{A2} are the resistances of Phase A1 and Phase A2:

$$\begin{cases} R_{\mathrm{A1}} = (1-\mu)R_{\mathrm{A}} \\ R_{\mathrm{A2}} = \mu R_{\mathrm{A}} \end{cases}. \tag{15}$$

Magnetic flux equa The inductance matrix $\boldsymbol{L}$ with ITSC fault in Eq. (7) is given by

$$\boldsymbol{L} = \begin{bmatrix} L_{\mathrm{A1A1}} & L_{\mathrm{A1A2}} & L_{\mathrm{A1B}} & L_{\mathrm{A1C}} & L_{\mathrm{A1a}} & L_{\mathrm{A1b}} & L_{\mathrm{A1c}} \\ L_{\mathrm{A2A1}} & L_{\mathrm{A2A2}} & L_{\mathrm{A2B}} & L_{\mathrm{A2C}} & L_{\mathrm{A2a}} & L_{\mathrm{A2b}} & L_{\mathrm{A2c}} \\ L_{\mathrm{BA1}} & L_{\mathrm{BA2}} & L_{\mathrm{BB}} & L_{\mathrm{BC}} & L_{\mathrm{Ba}} & L_{\mathrm{Bb}} & L_{\mathrm{Bc}} \\ L_{\mathrm{CA1}} & L_{\mathrm{CA2}} & L_{\mathrm{CB}} & L_{\mathrm{CC}} & L_{\mathrm{Ca}} & L_{\mathrm{Cb}} & L_{\mathrm{Cc}} \\ L_{\mathrm{aA1}} & L_{\mathrm{aA2}} & L_{\mathrm{aB}} & L_{\mathrm{aC}} & L_{\mathrm{aa}} & L_{\mathrm{ab}} & L_{\mathrm{ac}} \\ L_{\mathrm{bA1}} & L_{\mathrm{bA2}} & L_{\mathrm{bB}} & L_{\mathrm{bC}} & L_{\mathrm{ba}} & L_{\mathrm{bb}} & L_{\mathrm{bc}} \\ L_{\mathrm{cA1}} & L_{\mathrm{cA2}} & L_{\mathrm{cB}} & L_{\mathrm{cC}} & L_{\mathrm{ca}} & L_{\mathrm{cb}} & L_{\mathrm{cc}} \end{bmatrix}. \tag{16}$$

The self inductances are given by

$$\begin{cases} L_{\mathrm{A1A1}} = (1-\mu)L_{\mathrm{œs}} + (1-\mu)^2 L_{\mathrm{m}} \\ L_{\mathrm{A2A2}} = \mu L_{\mathrm{œs}} + \mu^2 L_{\mathrm{m}} \\ L_{\mathrm{BB}} = L_{\mathrm{CC}} = L_{\mathrm{m}} + L_{\mathrm{œs}} \\ L_{\mathrm{aa}} = L_{\mathrm{bb}} = L_{\mathrm{cc}} = L_{\mathrm{m}} + L_{\mathrm{œr}} \end{cases}. \tag{17}$$

The mutual inductances are given by

$$\begin{cases} L_{\mathrm{A1A2}} = L_{\mathrm{A2A1}} = \mu(1-\mu)L_{\mathrm{m}} \\ L_{\mathrm{A1B}} = L_{\mathrm{BA1}} = L_{\mathrm{A1C}} = L_{\mathrm{CA1}} = -\frac{1}{2}(1-\mu)L_{\mathrm{m}} \\ L_{\mathrm{A2B}} = L_{\mathrm{BA2}} = L_{\mathrm{A2C}} = L_{\mathrm{CA2}} = -\frac{1}{2}\mu L_{\mathrm{m}} \\ L_{\mathrm{A1a}} = L_{\mathrm{aA1}} = (1-\mu)L_{\mathrm{m}}\cos(\theta_{\mathrm{r}}) \\ L_{\mathrm{A1b}} = L_{\mathrm{bA1}} = (1-\mu)L_{\mathrm{m}}\cos(\theta_{\mathrm{r}} + \frac{2}{3}\pi) \\ L_{\mathrm{A1c}} = L_{\mathrm{cA1}} = (1-\mu)L_{\mathrm{m}}\cos(\theta_{\mathrm{r}} - \frac{2}{3}\pi) \\ L_{\mathrm{A2a}} = L_{\mathrm{aA2}} = \mu L_{\mathrm{m}}\cos(\theta_{\mathrm{r}}) \\ L_{\mathrm{A2b}} = L_{\mathrm{bA2}} = \mu L_{\mathrm{m}}\cos(\theta_{\mathrm{r}} + \frac{2}{3}\pi) \\ L_{\mathrm{A2c}} = L_{\mathrm{cA2}} = \mu L_{\mathrm{m}}\cos(\theta_{\mathrm{r}} - \frac{2}{3}\pi) \end{cases} . \tag{18}$$

The torque equation is given by

$$\begin{aligned} T_{\mathrm{e}} = & - n_{\mathrm{p}}L_{\mathrm{m}}[(i_{\mathrm{A}}i_{\mathrm{a}} + i_{\mathrm{B}}i_{\mathrm{b}} + i_{\mathrm{C}}i_{\mathrm{c}})\sin\theta_{\mathrm{r}} \\ & + (i_{\mathrm{A}}i_{\mathrm{b}} + i_{\mathrm{B}}i_{\mathrm{c}} + i_{\mathrm{C}}i_{\mathrm{a}})\sin(\theta_{\mathrm{r}} + \frac{2}{3}\pi) \\ & + (i_{\mathrm{A}}i_{\mathrm{c}} + i_{\mathrm{B}}i_{\mathrm{a}} + i_{\mathrm{C}}i_{\mathrm{b}})\sin(\theta_{\mathrm{r}} - \frac{2}{3}\pi)] \\ & + n_{\mathrm{p}}L_{\mathrm{m}}\mu i_{\mathrm{f}}[i_{\mathrm{a}}\sin\theta + i_{\mathrm{b}}\sin(\theta_{\mathrm{r}} + \frac{2}{3}\pi) \\ & + i_{\mathrm{c}}\sin(\theta - \frac{2}{3}\pi)]. \end{aligned} \tag{19}$$

The mechanical motion equation is not affected by the ITSC fault.

3 Wind Turbine Control under Generator Faults

Wind turbine control is one of the research focuses in the field of wind power. However, most of the research is on the control of wind turbines operating under normal conditions or grid fault conditions. With the development of offshore wind energy, the harsher environment of offshore wind farms and the need of reducing Levelized Cost of Energy (LCOE) from the industry made the research under faults more and more important. Under certain fault conditions, appropriate wind turbine control can reduce the fault impact and avoid the unscheduled shut-down. This chapter reviews generator faults and down-regulation strategies closely related to derating firstly. Then, the proposed fault treatments are introduced.

3.1 Generator Faults

The generator is one of the most critical components of a wind turbine, and its function is to convert the energy captured by the turbine into electrical energy. Therefore, the health condition of the generator is extremely important for wind turbines. Fig. 13 shows the normalised failure rates and downtimes for some main components in MW-class wind turbines [49]. It can be seen that the failure rate of the generator is not the highest, but the downtime of it is very long.

Generator faults and failures can be divided into electrical and mechanical categories. Common electrical faults include short circuit and open circuit of the stator winding and rotor winding, insulation damage, electrical imbalance, etc. Mechanical faults include: bearing failure, rotor mass imbalance, etc. [46]. Not all the impacts of these faults can be reduced by wind turbine control. As mentioned in Section I, some heat-related faults can be prevented from further developing by down-regulation to reduce the current heating at the early stage. The fault types studied in this thesis, generator cooling system fault and ITSC fault, are all heat-related faults. One of the main im-

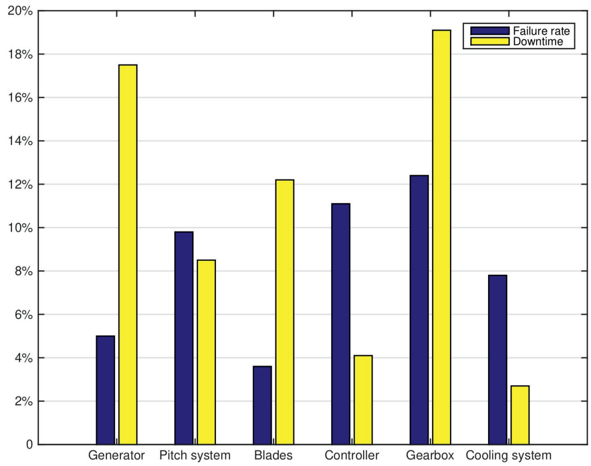

Fig. 13: Normalised failure rates and downtimes for some main components in MW-class wind turbines.

pacts of these two types of faults is the accelerated aging and damage of the winding insulation, and this impact on the insulating layer is a slow accumulation process. Therefore, the requirement of the response of the treatment is not as fast as some other serious electrical faults. The algorithm with a long calculating time can be used in this kind of application.

The research work in [47] showed the influence of the generator cooling system fault on the aging of the insulation layer through the electro-thermal analysis of DFIG. Stator ITSC is one of the most common faults of induction motors [8]. Typically, the percentage failure of the stator-related accounts for 38% of all the failure types of induction machines (see Fig. 14) [44]. Many other faults can be regarded as consequences caused by ITSC, such as phase-phase short-circuit and phase-ground short-circuit [55]. For the fault detection of the stator ITSC, there are many different ways. The research work [4] adopted Fast Fourier Transform of the stator instantaneous reactive power to detect the ITSC faults in stator and rotor windings. In the research work [14], the authors proposed a method that combined the Extended Park's Vector Approach (EPVA), the discrete wavelet transform and statistics to detect stator ITSC under transient conditions. In research work [51], ITSC fault was detected by analysing its rotor current and search-coil voltage.

Under the stator ITSC fault condition, the short-circuited part of the stator winding can be regarded as a new phase. The stator structure of DFIG has changed as shown in Fig. 12(a) and Fig. 12(b) [35]. Paper C calculates the power limitation based on this fault model. In the literature [36], the authors designed a closed-loop state observer to detect the ITSC fault. Paper D adopts

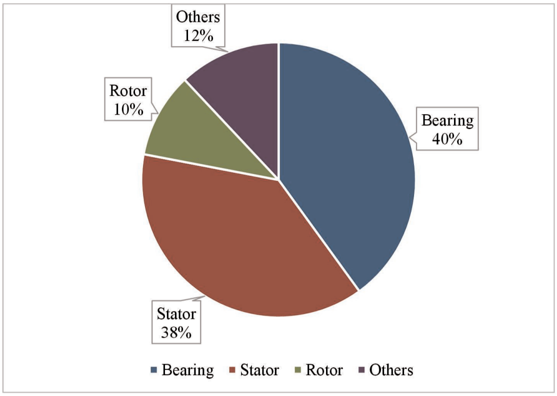

Fig. 14: Percentage failure by components in induction machines.

this detection method for the ITSC fault ride-through strategy.

3.2 Down-Regulation

Down-regulation is an operation mode of wind turbines. Wind turbines do not convert the available wind energy into electrical energy as much as possible. The power reference of the wind turbine is smaller than the value on the power curve of wind turbines corresponding to the current wind speed. Since the penetration of wind power in the grid increases rapidly, the grid has more requirements for wind turbines and wind farms [53]. Down-regulation mode is necessary to reserve power according to the command from the grid. In [39], three down-regulation strategies, namely Max-ω, Constant-ω and Constant-λ were compared and discussed. Max-ω strategy can store the kinetic energy in the rotating rotor and react quickly when the grid needs more power. These three strategies were also compared in [38]. Because the static operating point has the smallest C_t, the wind farm which adopts Constant-ω strategy can produce the most power. The research work [28] studied the effect of different down-regulation strategies for reducing the fatigue loads of the wind turbine components. The results showed that all these strategies can reduce the fatigue loads of some of the components. The specific effects vary according to the different operating conditions.

Based on the analysis of wake effects, it can be seen that the smaller C_t of the upstream wind turbine will lead to the higher wind speed of the downstream wind turbine. Therefore, Paper E proposes a Min-C_t down-regulation strategy. When wind turbines get the down-regulation command, the controller will calculate the appropriate operating point. Then through the torque control and the pitch control, wind turbines will operate at the

Minimum thrust coefficient status.

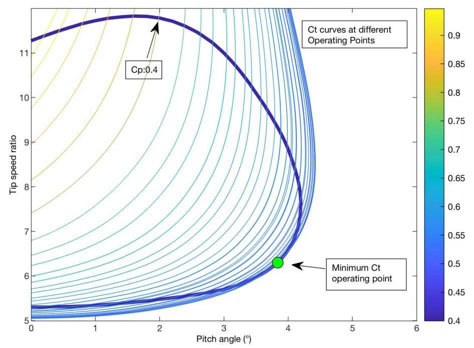

Fig. 15: C_p curve with different operating points and C_t values.

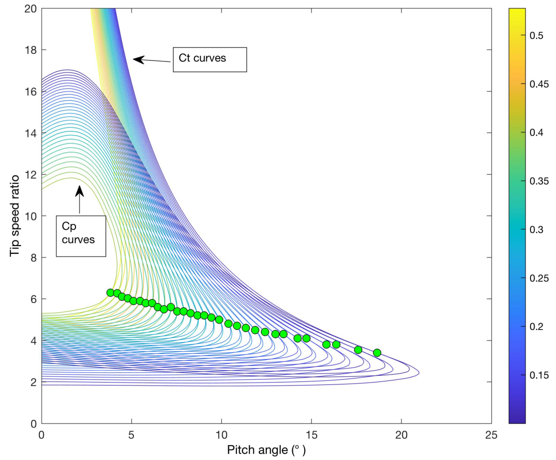

Fig. 16: Min-C_t operating points on C_p curves.

When the wind turbine is running in the down-regulation mode, the value of C_p of the wind turbine should be smaller than the value that the wind turbine can achieve to reduce the power output. As seen in Fig. 15, all the operating points on the dark blue curve have the same C_p. But the values of C_t at different operating points are different. The purpose of Min-C_t down-regulation strategy is to select the operating point with minimum C_t from the C_p curve under the constraint conditions. The green circle in Fig. 15 shows the Min-C_t operating point when C_p is 0.4.

Table 1: Comparison of different down-regulation strategies.

Variables	Max-ω	Min-C_t
P	1.43 MW	1.43MW
β	3.85°	4.21°
ω_r	1.267	0.788
C_p	0.3891	0.3884
C_t	0.5775	0.5074
v_{down}	6.72 m/s	6.91 m/s
P_{down}	0.99 MW	1.08 MW
ΔP_{down}	0	9.09 %

According to the Min-C_t strategy, the operating curve can be obtained through marking the minimum C_t operating points on the C_p curve of different values. The green circles in Fig. 16 are the Min-C_t operating points when C_p is from 0.1 to 0.4. The corresponding C_t curves are also displayed.

Paper E compares Max-ω strategy and Min-C_t strategy when the power of the upstream wind turbine is down-regulated from 1.79 MW to 1.43 MW. The simulation results in Paper E are shown in Tab. 1, where P, β, ω_r, C_p, and C_t are the power output, pitch angle, mechanical rotor speed, power coefficient, and thrust coefficient of the upstream wind turbine respectively. $v_{down}$and P_{down} are the wind speed and the power output of the downstream wind turbine respectively. ΔP_{down} is the percentage of the power change.

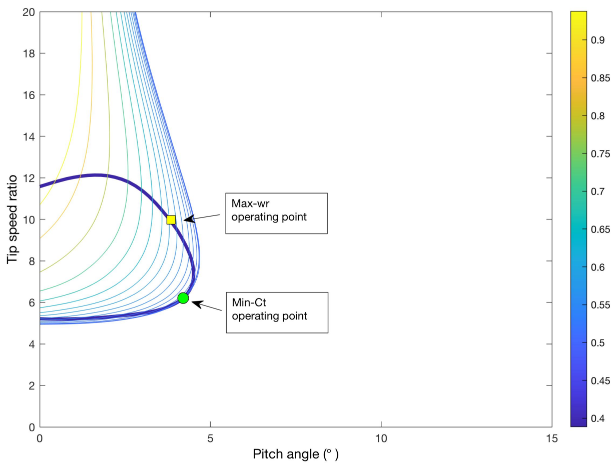

Fig. 17: Comparison of the operating points in Max-ω and Min-C_t strategy.

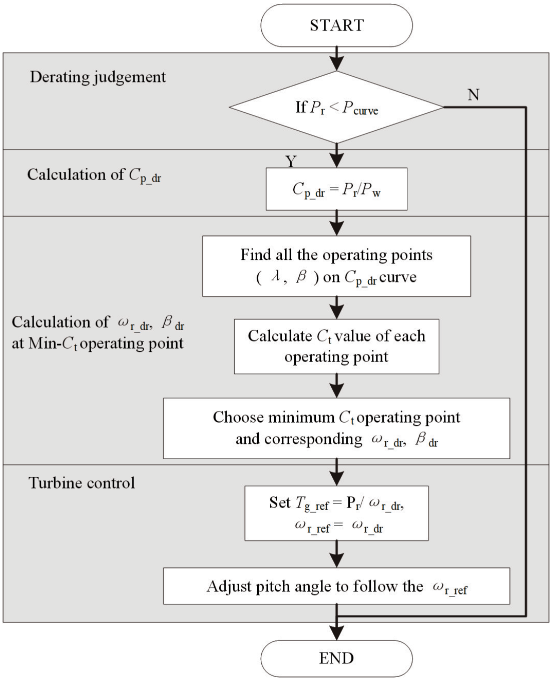

Fig. 18: Flowchart of Min-C_t strategy.

It can be seen that in the Min-C_t strategy, the C_t of the upstream wind turbine is smaller.

The wind speed and the power of the downstream wind turbine are greater. Fig. 17 shows the operating points of the upstream wind turbine under different strategies.

The flowchart of Min-C_t strategy is shown in Fig. 18, where P_{curve} is the power value corresponding to the current wind speed on the power curve; C_{p_dr} is the C_p that needs to be derated; P_w is the power of the wind that inflows to the swept area of the rotor; ω_{r_dr} is the rotor speed that needs to be set in the derating mode; β_{dr} is the pitch angle that needs to be set in the derating mode; T_{g_ref} is the generator torque reference; ω_{r_ref} is the rotor speed reference.

Min-C_t strategy is also used on healthy wind turbines for improving the wind farm power in Paper F. Paper F compares Min-C_t strategy with Max-ω strategy in a larger operating range by simulation. The range of power reference is from 2 MW to 5 MW. The range of wind speed is from 3 m/s to 14 m/s. The surfaces of $\Delta\omega$ and ΔC_t are presented to show the difference between two strategies in Fig. 19 and Fig. 20.

The definitions of $\Delta\omega$ and ΔC_t are shown as follows.

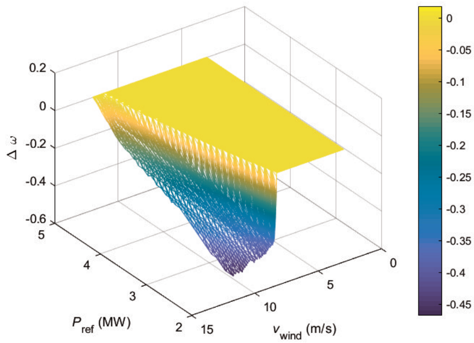

Fig. 19: $\Delta\omega$ between Min-C_t strategy and Max-ω strategy.

$$\begin{cases} \Delta\omega = \omega_{\_Min-C_t} - \omega_{\_Max-\omega} \\ \Delta C_t = C_{t\_Min-C_t} - C_{t\_Max-\omega}, \end{cases} \tag{20}$$

where $\omega_{\_Min-C_t}$ and $\omega_{\_Max-\omega}$ are the rotor speeds under Min-C_t and Max-ω strategies; $C_{t\_Min-C_t}$ and $C_{t\_Max-\omega}$ are the thrust coefficients under Min-C_t and Max-ω strategies.

From Fig. 19, it can be seen that the difference of ω between two down-regulation strategies is significant in the area of high wind speed and low power reference.

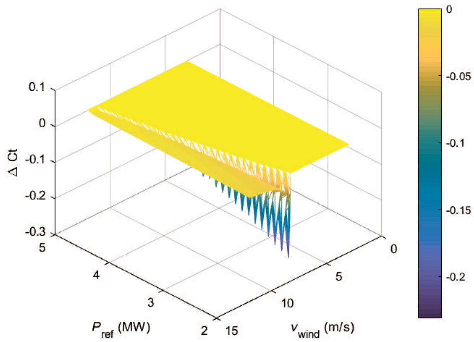

Fig. 20: ΔC_t between Min-C_t strategy and Max-ω strategy.

Fig. 20 shows the difference of C_t under different down-regulation strategies. The trend of ΔC_t is different from that of $\Delta\omega$. When the upstream wind turbines are in the area that ΔC_t is negative, the power of the wind farm is possible to be improved by adopting Min-C_t strategy.

Table 2: Wind farm power with different strategies

Derating strategy Dispatch strategy	Max-ω PDS $\boldsymbol{P}$(MW)	Max-ω OPDS $\boldsymbol{P}$(MW)	Min-C_t OPDS $\boldsymbol{P}$(MW)
WT1	5.00	5.00	5.00
WT2	4.17	3.72	3.70
WT3	3.11	3.31	3.30
WT4	2.84	3.41	3.40
WT5	2.76	3.40	3.56
P_{WF}	17.88	18.84	18.96

The simulation was made in Paper F to compare the impacts of these two down-regulation strategies on wind farms. The wind speed is 12 m/s, and the power demand of the wind farm is 20 MW. The comparison was made between different active power dispatch strategies and different down-regulation strategies, where PDS is the proportional dispatch strategy, OPDS is the optimal power dispatch strategy, WT1 to WT5 represent five wind turbines in the wind farm. The layout is shown in Fig. 10. The simulation results are shown in Tab. 2 and Fig. 21. Here, we can only focus on the last two columns.

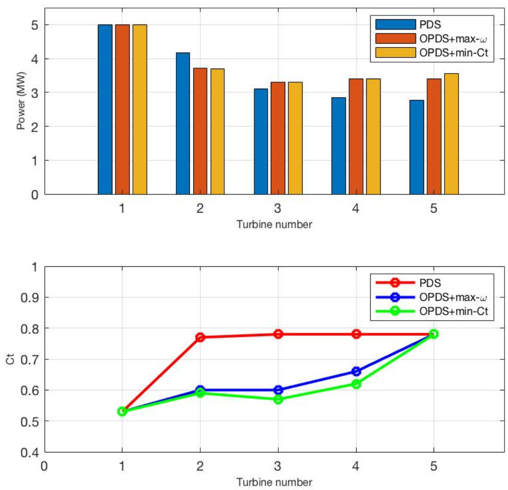

Fig. 21: Power output and C_t under different strategies.

As shown in Fig. 21, the values of C_t in Min-C_t are smaller than that in Max-ω strategy. These differences lead to the increase of the wind farm power output.

3.3 Fault Treatment

Wind turbines have a higher failure rate comparing with steam/hydro/gas turbines in the traditional power plant [46]. Therefore, reasonable fault treatment is more important for wind turbines. Paper A classifies the wind turbine generator faults into three levels: minor faults, medium faults and severe faults. Minor faults may be caused by wind speed fluctuation, grid disturbance, temporary wrong sensor reading, etc. The faults in this level can be cleared by temporary shut-down or restart [46]. For the severe faults, the faulty turbine must be shut down. What needs to be studied is medium faults.

Several research works have shown that some impacts of the faults of generators can be reduced by derating. Literature [16] adopts derating the squirrel-cage induction motor under rotor broken bars fault. In [29], the three-phase induction motor under unbalanced voltages is derated to avoid excessive heating. In [5], the authors estimated machine currents and developed torque of multiphase machines under open circuit phase(s) based on the steady-state model and avoid the increase of DC-link voltage by derating. The common point of these research works is to reduce the fault effects by derating. This thesis also adopts this idea for the cooling system fault and stator ITSC fault. The key to derating is to find the right degree, or named the derating factor, to prevent the faulty generator from further damage.

Paper A takes the wake effect into account and tries to meet the power demand from TSO on the premise that the power of the faulty wind turbine does not exceed the power limitation. If the healthy wind turbines can generate enough power, the faulty wind turbine will be shut down. The flowchart of the proposed active power dispatch strategy is shown in Fig. 22, where $P_{\mathrm{r},i}$ is the power reference of the i^{th} wind turbine; $P_{\mathrm{a},i}$ is the available power of the i^{th} wind turbine; $P_{\mathrm{a,h},i}$ is the available power of the i^{th} healthy wind turbine; $P_{\mathrm{a,f},i}$ is the available power of the i^{th} faulty wind turbine; $P_{\mathrm{r,f},i,min}$ is the minimum power reference that should be set on the i^{th} faulty wind turbine for tracking the power demand; $P_{\mathrm{limit},i}$ is the power limitation of the i^{th} faulty wind turbine.

FL1 represents minor faults; FL2 represents medium faults; FL3 represents severe faults. The active power dispatch method is proportional power dispatch strategy. The explanation of this strategy is given in Sec. 4.1. Since this strategy does not take wake effect into account, the power output of wind farms needs to be estimated before derating for FL2 for tracking the power demand as much as possible. If the healthy wind turbines can meet the

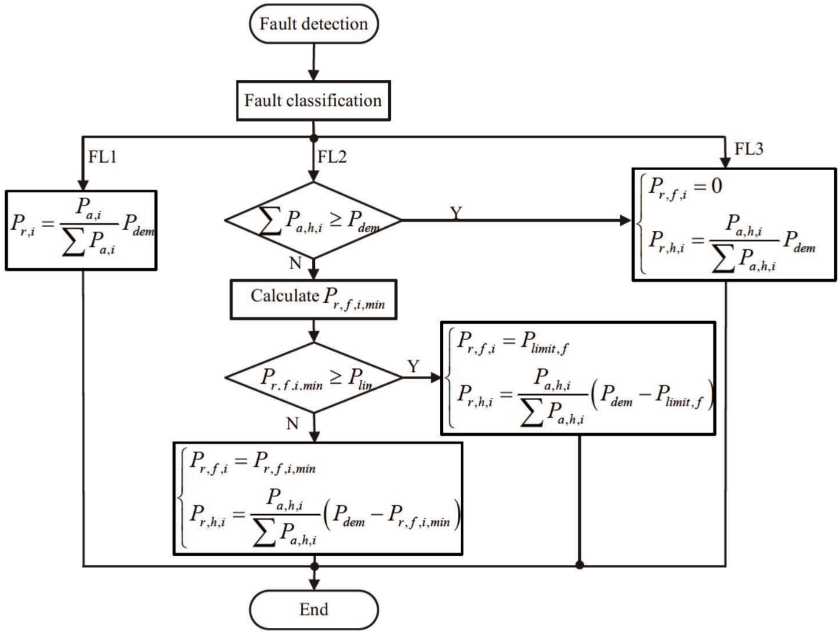

Fig. 22: Flowchart of the active power dispatch strategy in Paper A.

power demand, the faulty turbine can be shut down. If the sum of the total power from the healthy wind turbines and the power limitation of the faulty wind turbine is smaller than the power demand, the power limitation will be set as the power reference to the faulty turbine. That means the wind farm cannot meet the power demand for protecting the faulty turbine. Otherwise, the power reference of the faulty turbine can be set as the difference between the power demand and the total power from the healthy wind turbines.

The fault type mentioned in Paper B is the generator cooling system fault. The fault model has been described in Sec 2.4. It can be seen that the thermal resistance R_{th} is the main parameter that affects the temperature rise. The higher the degree of fault, the greater the value of R_{th}. The specific values of the parameters can be estimated from actual measured data. In Paper B, R_{th} is assumed to be 0.003 K/W under normal conditions. According to the power loss of the generator under different power, the temperature rise curve under different R_{th} can be obtained, as shown in Fig. 23.

To ensure that the faulty wind turbine operates safely under the faulty condition without exceeding the temperature rise under normal condition, the power output of the generator needs to be limited to the power corresponding to the maximum allowable temperature rise on different curves. In the simulation in Paper B, the wind speed is 12 m/s and the power demand of the wind farm is 18 MW. The generator cooling system fault occurs on

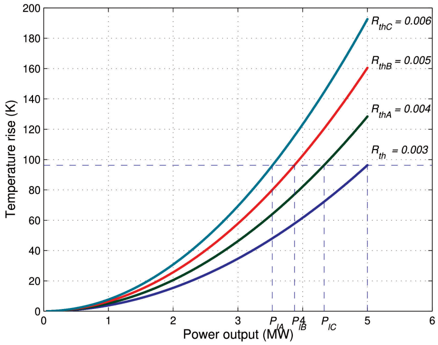

Fig. 23: Temperature rise curves under different thermal resistances.

wind turbine WT2. The impact of the fault is that R_{th} increases from 0.003 K/W to 0.006 K/W.

Fig. 24 shows the temperature rise of the faulty wind turbine and the power output of the wind farm under different fault treatment methods, where M1 represents that the faulty wind turbine continues to operate according to the original strategy; M2 represents that the faulty wind turbine directly shuts down; M3 represents the derating strategy proposed by Paper B. It can be seen that although strategy M1 does not affect the power output of the wind farm, the temperature rise exceeds the allowable value. In practice, when the faulty current exceeds the safe current value, the safety alarm will be triggered and the wind turbine will be shut-down directly. So Strategy M1 is only used to analyse the impact of the fault treatment on wind turbines and the wind farm. Strategy M2 protects the faulty unit, but it greatly reduces the power output of the wind farm. Strategy M3 not only protects the faulty wind turbine and also maintains the power output of the wind farm.

Paper C considers the ITSC fault in the stator winding. The fault treatment strategy is similar to that in Paper B. The difference is the calculation of the power limitation. First, the fault current should be calculated with respect to power and fault level according to the fault model mentioned in Sec. 2.5. Then, the fault current surface can be obtained as shown in Fig. 25.

Fig. 25. shows that the rated current surface divides the fault current surface into two parts: the part below the rated current surface indicates that the fault current will not exceed the rated current within this power and fault level range; the other part indicates that the fault current will exceed the rated current. To ensure that the generator can continue to operate safely at a specific fault level, the power output of the faulty generator should be limited to the power value corresponding to the intersection of the fault current surface

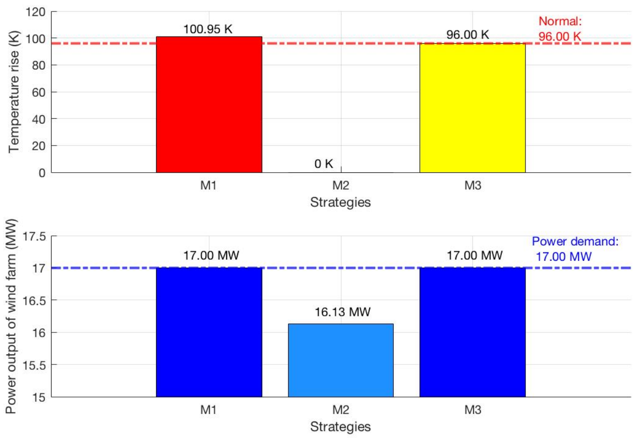

Fig. 24: Comparison of temperature rise and power output of wind farm under different fault treatment strategies.

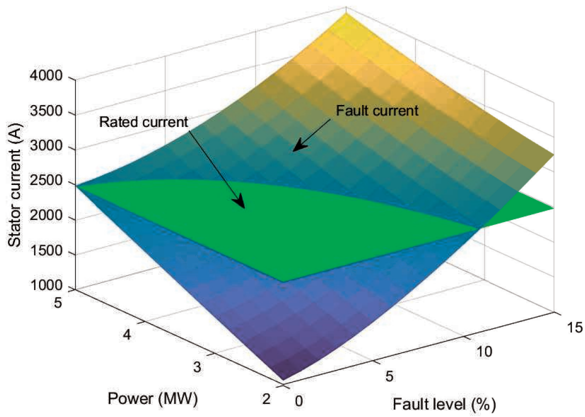

Fig. 25: Fault current surface.

and the rated current surface. This intersection is the power limitation curve as shown in Fig. 26.

For ITSC fault, Paper D adopts another treatment which is ITSC fault ride-through strategy. After the ITSC fault is detected, Paper D superimposes a PI control-based correction value on the original torque reference or pitch angle reference according to the specific operating condition of the wind turbine. The flowchart in Fig. 27 details this ITSC fault ride-through strategy.

Compared with the treatment strategy in Paper C, ITSC fault ride-through

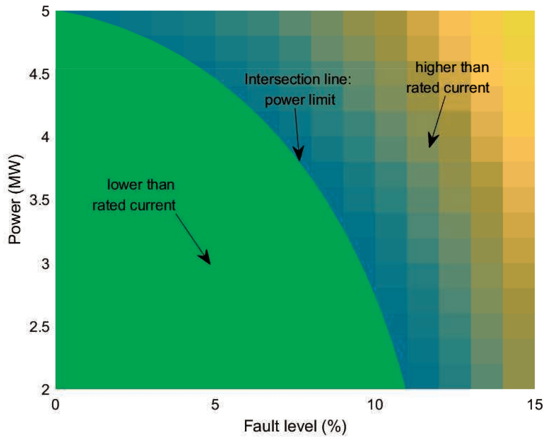

Fig. 26: Power limitation curve.

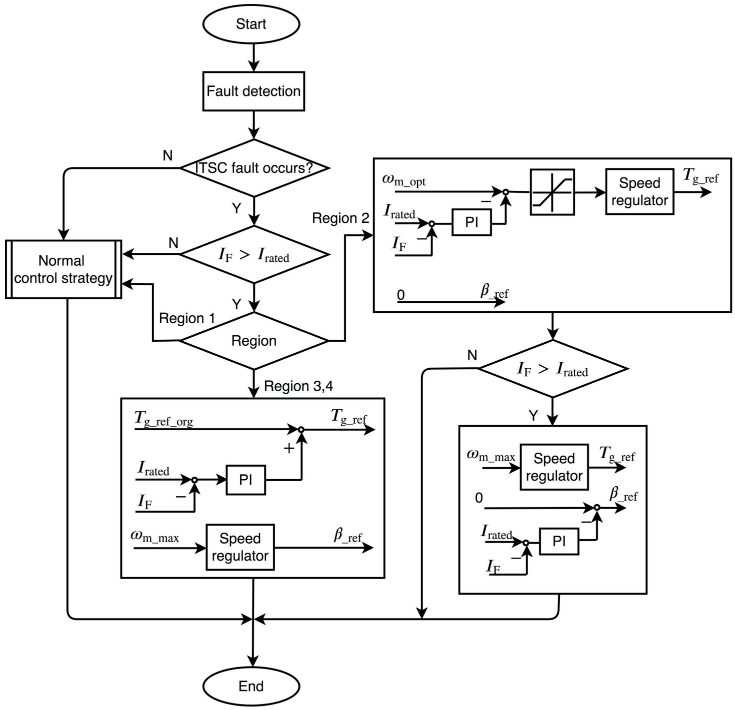

Fig. 27: Flowchart of ITSC fault ride-through strategy.

strategy avoids the problem of the inappropriate fault limitation caused by the inaccurate fault level estimation. The derating command is sent at the turbine level, not the wind farm level. The change of the effective current of the faulty phase is shown in Fig. 28. The ITSC fault occurs in Phase A at t = 30 s. ITSC fault ride-through strategy is activated at t = 35 s to show the effect of the strategy more clearly. The results show that the effective current of the faulty phase returns to the rated value in less than 10 seconds. Since the impact of ITSC fault on the temperature is a large inertia process, this recovery time is completely acceptable.

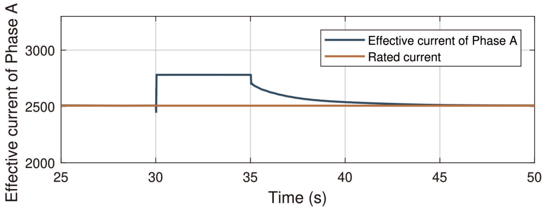

Fig. 28: Effective current of the faulty phase.

4 Wind Farm Power Optimization

Different from conventional power plants with controllable motive power, the wind energy passing through the wind farm is not stable. In addition, a wind farm consists of multiple wind turbines, and the aerodynamic interaction directly affects the available power of wind turbines. From the perspective of the grid, it would be best if a wind farm can operate as a conventional power plant. Therefore, the wind farm needs to coordinate all wind turbines to meet the requirements from TSO. When faults occur on wind turbines, the wind farm should be able to reduce the impacts of faults through reasonable control so that the overall characteristics of wind farms will not be affected too much. Since the method of this thesis protects the faulty generator by derating the faulty wind turbine, the impact of the corresponding treatment for wind farms is the reduction of the power generation capacity. To reduce this negative impact due to the protection, the power capacity of wind farms should be improved. This chapter summarizes the power dispatch method and active wake control of wind farms.

4.1 Power Dispatch Strategy

The basic function of power dispatch is to allocate reasonable power references to all the wind turbines to meet TSO's requirements for the wind farm. The simplest power dispatch strategy is to evenly distribute the power demand to each wind turbine [19]. The power references for wind turbines can be given by

$$P_{\mathrm{r},i} = \frac{P_{\mathrm{dem}}}{n}, \tag{21}$$

where $P_{\mathrm{r},i}$ is the power reference of the ith WT; P_{dem} is the power demand from TSO.

Compared with this simple strategy, the proportional dispatch strategy proposed in [12] is more reasonable, which distributed the power demand to all wind turbines according to their available power ratio. Because the proportional dispatch strategy takes the low available power of the downstream wind turbines caused by wake effects. The power references for wind turbines can be calculated by

$$P_{\mathrm{r},i} = \frac{P_{\mathrm{a},i}}{\sum_{i=1}^{n} P_{\mathrm{a},i}} P_{\mathrm{dem}}, \tag{22}$$

where $P_{\mathrm{a},i}$ is the available power of the ith WT. However, the proportional dispatch strategy only realizes the power distribution for wind farms.

In addition, many studies achieved basic function while taking into account other optimization objectives. In [15], the authors proposed a wind farm control system with a hierarchical structure with both a central control level and a local control level to minimize the destructive fluctuation of torque and generator speed. Three optimal power dispatch models were proposed in [58] to reduce the blade damage and the generator losses. In [34], the authors distributed the power demand according to the inverse proportion of the fatigue of wind turbines to optimize the fatigue distribution of wind farms. An optimal dispatch strategy was proposed to minimize the internal wind grid loss and complied with the requests from TSO [12]. In [26], the authors proposed a priority classification model of wind turbines to decrease the line losses of the collection system in wind farms. Most of these studies adopt optimization algorithms to achieve multi-optimization. The key is the representation of the objectives in the objective function.

In this thesis, the power dispatch strategy proposed in Paper A is based on the proportional power dispatch strategy, the static model of the wind farm, and the severity of the fault. In paper B, C and F, the proposed power dispatch strategy calculates the power references of wind turbines based on the static model of the wind farm and the PSO algorithm to optimize the total power of the wind farm and reduce the power loss caused by the protection of the faulty wind turbine. The optimization methods in Paper B and Paper C are the same. The objectives include the following items:

- Protecting the faulty wind turbine.
- Tracking the power demand from TSO.
- Minimizing the power loss caused by wake effects.
- Minimizing the power fluctuation.

As the most important objective, protecting the faulty wind turbine will be used as the constraint. The other items will be treated as the optimization objectives. The active power dispatch schedule can be organized as a constrained multi-objective optimization problem. The objective function is given by

$$\begin{aligned}
\min & \frac{|\sum_{i=1}^{n} P_i(k) - P_{\text{dem}}(k)|}{P_{\text{dem}}(k)} \cdot k_1 + \{1 - \mathrm{r}[\boldsymbol{P}(k-1), \boldsymbol{P}(k)]\} \cdot k_2 \\
& + \frac{\sum_{i=1}^{n} |P_{\mathrm{r},i}(k) - P_i(k)| / P_{\mathrm{r},i}(k)}{n} \cdot k_3 \\
s.t. & \begin{cases} 0 \le P_{\mathrm{r},i}(k) \le P_{\text{rated}}, & i^{th} \text{ wind turbine is healthy,} \\ 0 \le P_{\mathrm{r},i}(k) \le P_{\text{limit}}, & i^{th} \text{ wind turbine is faulty,} \end{cases}
\end{aligned} \tag{23}$$

where, n is the number of wind turbines, $P_{\mathrm{r},i}(k)$ is the power reference of the i^{th} wind turbine at time k; $P_i(k)$ is the power output of the i^{th} wind turbine at time k; $\boldsymbol{P}(k)$ is the power output vector at time k, $P_{\text{dem}}(k)$ is the power demand from TSO at time k; P_{rated} is the rated power of the wind turbine; P_{limit} is the power limitation of the faulty wind turbine.

It can be seen that the power limitation is set as the upper limit of the power reference of the faulty wind turbine in the constraint. The objective function includes three items. The first item represents that the total power of all the wind turbines should track the power demand from TSO.

The second item is the correlation coefficient of $P_i(k)$ and $P_i(k-1)$ subtracted by one. It can represent the power fluctuation between two adjacent moments. If the value of this term is zero, that means no power fluctuation. The calculation of PSO includes a random process. Therefore, if the power fluctuation caused by the power reference is not taken into account, the optimization results at the two adjacent moments may be quite different and lead to an excessive power change of the individual wind turbine. The expression of the correlation coefficient is given by

$$\mathrm{r}[\boldsymbol{P}(k-1), \boldsymbol{P}(k)] = \frac{\mathrm{cov}[\mathbf{P}(k-1), \boldsymbol{P}(k)]}{\mathrm{std}[\boldsymbol{P}(k-1)] \cdot \mathrm{std}[\boldsymbol{P}(k)]}, \tag{24}$$

where $\mathrm{cov}[\mathbf{P}(k-1), \boldsymbol{P}(k)]$ is the covariance of $P_i(k)$ and $P_i(k-1)$; $\mathrm{std}[\boldsymbol{P}(k-1)]$ and $\mathrm{std}[\boldsymbol{P}(k)]$ are the standard deviations of $P_i(k)$ and $P_i(k-1)$.

The third item represents the differences between power reference and the power output of all the wind turbines. Since the power that wind turbines can produce cannot exceed the available power, the wind turbine will produce the same power output when it receives all the power references greater than the available power. If this feature of wind turbines is not considered in the PSO optimization process, the optimization may fall into a local optimum. The structure of the active power dispatch strategy in Paper B and Paper C is shown in Fig. 29.

The simulation is made to compare the proportional dispatch strategy and the optimal power dispatch strategy. When the wind speed is 12 m/s and

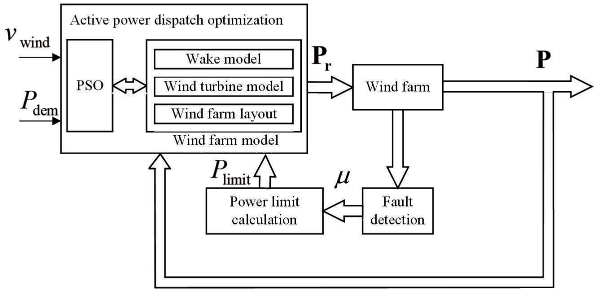

Fig. 29: Structure of wind farm power dispatch in Paper B and Paper C.

the power demand is 18 MW. The result is shown in Tab. 3, where PDS is proportional dispatch strategy; OPDS is optimal power dispatch strategy; $\boldsymbol{P}_{\mathbf{r}}$ is the power reference vector of wind turbines; $\boldsymbol{P}$ is the power output vector of wind turbines. It can be seen that OPDS can make the wind farm produce more power because of the consideration of wake effects.

Table 3: Comparison of power generation capacity between PDS and OPDS

	PDS		OPDS	
	$\boldsymbol{P}_{\mathbf{r}}$(MW)	$\boldsymbol{P}$(MW)	$\boldsymbol{P}_{\mathbf{r}}$(MW)	$\boldsymbol{P}$(MW)
WT1	5.00	5.00	5.00	5.00
WT2	4.20	4.17	4.17	4.17
WT3	3.13	3.11	3.01	3.01
WT4	2.86	2.84	3.00	3.00
WT5	2.78	2.76	2.81	2.81
P_{WF}	18.00	17.88	18.00	18.00

To verify the effect of the second item in the objective function, another simulation is made. In this simulation, the power demand changes from 17 MW to 16 MW. The values of k_2 are set to 0 and 4, respectively. The result is shown in Tab. 4 and Fig. 30.

It can be seen that although when k_2 takes different values, the power output of the wind farm can track the power demand very well, the power reference varies greatly. When $k_2 = 4$, the change of the power references is small, which can avoid the excessive power fluctuation of wind turbines.

With respect to the calculation time, the fidelity of the wake model dominates the computational cost of the optimization process. The analytical model is more suitable for wind farm optimization computing because of its low computational cost ($\sim 10^{-3}$ CPU hours per simulation) [45]. The iteration number and the population size adopted here are 50 and 60 respectively.

Table 4: Comparison of power fluctuation in OPDS

	$k_2 = 0$		$k_2 = 4$	
	$\boldsymbol{P}$(MW)	$\boldsymbol{P'}$(MW)	$\boldsymbol{P}$(MW)	$\boldsymbol{P'}$(MW)
P_{dem}	17.00	16.00	17.00	16.00
WT1	5.00	4.82	5.00	5.00
WT2	4.17	4.25	4.17	4.17
WT3	2.81	2.01	2.81	2.51
WT4	2.61	1.51	2.61	2.21
WT5	2.41	3.41	2.41	2.11
P_{WF}	17.00	16.00	17.00	16.00
$\text{r}(\boldsymbol{P}, \boldsymbol{P'})$	0.8161		0.9987	

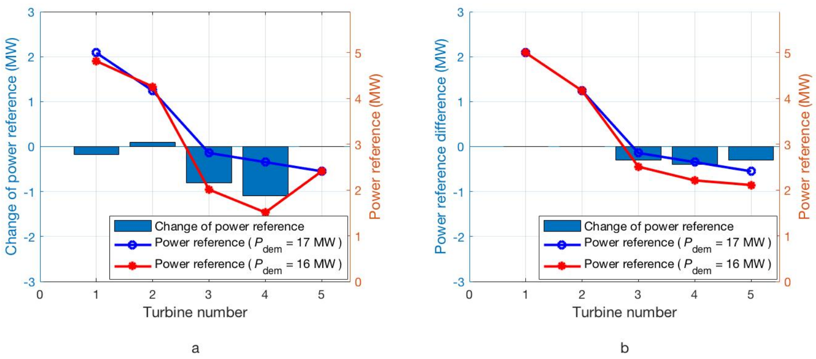

Fig. 30: Comparison of power fluctuation (a) Power reference and its change ($k_2 = 0$), (b) Power reference and its change ($k_2 = 4$).

The calculation time for five wind turbines case is about 4 seconds with Intel i5 2.8GHz CPU. With faster CPU and parallel computing, the calculation time can be further reduced. The power reference update time of the practical wind farms varies from seconds to minutes.

Different from Paper B and Paper C, Paper F adopts the ITSC fault ride-through strategy at the turbine level to protect the faulty generator. Therefore, the power dispatch method in Paper F does not need to consider the fault condition. From the case study in Paper F, it can be seen that the estimated fault level will directly impact the final derating. If the estimated fault level is higher than the actual fault level, the faulty wind turbine will be over-reduced. If the estimated fault level is lower than the actual fault level, the faulty phase current will be greater than the rated current. Without the use of the power limitation, the inaccurate derating due to the estimation error of the fault level can be avoided as well.

The structure of the wind farm power dispatch strategy is shown in Fig. 31.

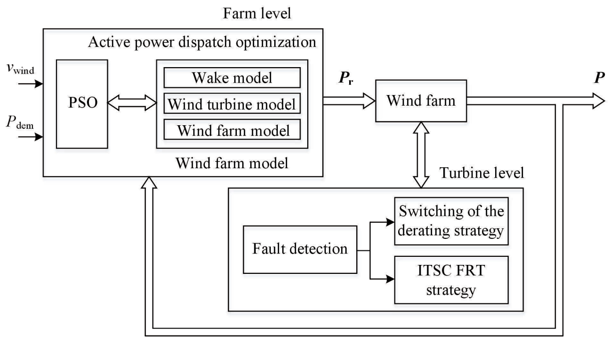

Fig. 31: Structure of wind farm power dispatch strategy in Paper F.

4.2 Active Wake Control

The wake effect is an unavoidable problem in wind farm power optimization and maximization. Due to wake effects, maximizing the power of a single wind turbine will not maximize the total power of wind farms. Wake effects can reduce the total power of wind farms by up to 54% [41]. And the revenue losses can reach 20 to 30% [10]. Especially in the case of faulty wind turbines operating with power limitation, wind farm power control that takes the operating conditions of the faulty wind turbine into account is even more important. Unlike wind farm layout optimization and other optimizations carried out at the design stage, the power of existing wind farms can be improved through wind turbine control and wind farm control. At present, there are two mainstream concepts for increasing the power of wind farms by active wake control, one is axial induction-based control, and the other is yaw-based control.

Axial induction-based control This is a concept proposed quite early [54]. Axial induction factor is related to the power and the thrust coefficient of the wind turbine rotor and is a measure used to express the momentum deficit of the air flowing through the wind turbine rotor [30]. When the upstream wind turbine reduces the axial induction factor by reducing the power and thrust coefficient, the downstream wind turbine is expected to obtain a higher wind speed. If the power increase of the downstream wind turbines can be greater than the power reduction of the upstream wind turbines, then the overall power of the wind farm can be improved. In [50], the power of the upstream wind turbine was reduced by deviating the pitch angle from the optimal value. In [24], the authors obtained a power increase of 2.85% by adjusting the tip speed ratio below the rated wind speed. Paper E proposes a minimum C_t strategy to reduce the C_t of the upstream wind turbine. Paper F applies the minimum C_t strategy to wind turbines and combines power dispatch optimization to achieve wind farm power optimization.

Additionally, distributed algorithms are also used to improve wind farm power. Compared with the greedy algorithm that adjusts the axial induction factor to the optimal value, the power has been greatly improved under the steady-state and constant wind conditions through the model-free distributed learning algorithm [37]. In [21], the authors also adopted a distributed algorithm based on the information of nearby wind turbines and then improved the power of the wind farm through a gradient-based optimization algorithm.

However, some recent studies have shown that it is difficult to really increase the overall power of wind turbines in CFD simulation and practice by optimizing the axial induction factor based on engineering models [7, 13]. Because the wind speed on the wake section is not evenly distributed. As seen in Fig. 32, the part with the highest wind speed is at the edge of the wake, which is not in the swept area of the rotor of the downstream wind turbine. In addition, the derated upstream wind turbine also reduces the turbulence in the wake. This will lead to a reduction in wake expansion and momentum recovery [30].

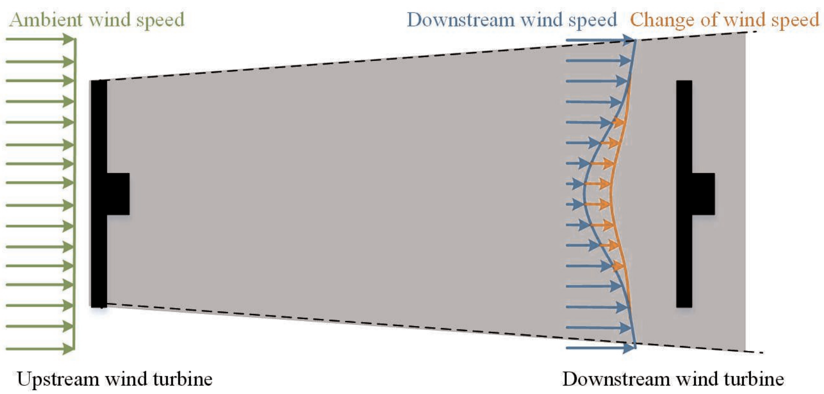

Fig. 32: Wake condition in axial induction-based control concept.

Yaw-based control Typically, the rotor of the wind turbine should face the direction of the inflow wind to extract the maximum energy. The wake condition in yaw-based control concept is shown in Fig. 31. However, the concept of the yaw-based control is to steer the direction of the wake through the yaw misalignment of the upstream wind turbines, so as to prevent the downstream wind turbines from being in the low wind speed area of the wake. This approach is different from the original design of the wind turbine, but it has the potential to reduce the wake effect. In recent years, more and more researchers have adopted this concept to improve the power of wind farms [20, 25]. The effectiveness of yaw-based control has been verified both in wind tunnel test [9] and large-eddy simulation [17].

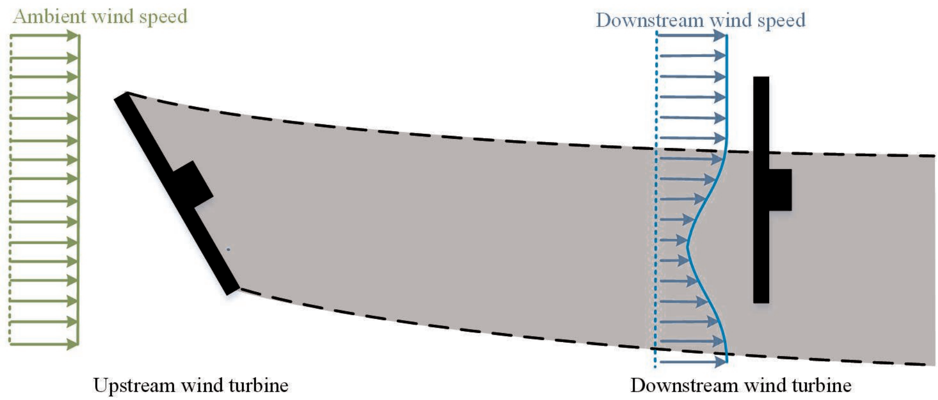

Fig. 33: Wake condition in yaw-based control concept.

In [18], authors employed the yaw-based wake steering in a commercial wind farm. This yaw off strategy calculated the optimal yaw deviation value for wind speed and wind direction in the engineering model and then saved them in a look-up table. A wake deflection controller was designed to provide a nacelle vane signal with optimized deviation to the yaw controller. The inputs of the wake deflection controller are the sensor signals of the wind turbine, and the output is the modified nacelle vane signal. The test results showed that for the two adjacent wind turbines, the power of the downstream wind turbine in 10° sector increased by 14%, and the total power of the upstream and downstream wind turbines increased by 4%.

However, it should be noted that the method based on yaw-based control requires accurate control of yaw, which raises the requirements for wind direction diagnosis. The wrong yaw deviation may result in a decrease in the total power of wind turbines. It is difficult to get an accurate wind direction estimation based on the anemometer and vane mounted on the nacelle, and the use of LIDAR equipment will increase the costs. The methods based on wake redirection may also respectively lead to an increase of fatigue loads on the blades and drive chain [31].

In addition to these two mainstream concepts, there are also some novel concepts such as nacelle tilt and turbine reposition [17]. However, at present, wind turbines with adjustable nacelle tilt degree are not available, and there are only a few floating wind turbines.

5 Closing Remarks

5.1 Conclusions

This thesis studied the offshore wind farms under generator faults, including analysis of fault models, control at turbine level and optimization at farm level. For different levels of the generator faults, Paper A proposed different treatments on the premise of protecting the faulty wind turbine and minimizing the impact of the fault. For heat-related faults that do not have a significant impact on the wind turbine at the initial stage of the fault, the faulty wind turbine was derated instead of operating as normal or shutting down. This strategy was also adopted in Paper B, C and F.

Paper B analysed the simplified fault model of the generator cooling system, and then restricted the power of the faulty wind turbine in the active power dispatch optimization. Both Paper C and F studied the stator ITSC fault of DFIG. Through the study of the fault model, the faulty wind turbine was restricted according to the fault level. Paper F adopted the ITSC fault ride-through strategy proposed by Paper D to limit the power of the faulty wind turbine at the turbine level. The advantage is that the estimation of the fault level is not necessary any more, and there is no need to consider the fault conditions in the power dispatch optimization. To further reduce the power loss caused by the faulty wind turbine, Paper E proposed the Min-C_t strategy suitable for healthy wind turbines to reduce the wake effect.

As mentioned in Paper A, simply choosing to shut down or continue to operate as normal is not appropriate for both the wind farm and the faulty wind turbine without considering the fault severity. On the premise that the fault can be accurately diagnosed, corresponding treatments should be implemented for different types of faults. In this way, compared with direct shutting down, the wind turbine with minor faults can avoid unnecessary power loss. Compared with continuing to operate as normal, the wind turbine with serious faults can be protected well. The active power dispatch strategy proposed by Paper A can consider the fault level, power demand and wake effects to dispatch the power references reasonably. It can avoid the neglect of fault and excessive protection, and provide a reasonable solution for wind farm operation under fault. In this way, for some faults that the impact of the fault can be estimated, the faulty wind turbine can be protected with the least power cost.

For specific generator faults, the method proposed by Paper B can obtain the corresponding power limitation with known fault model parameters, and protect the faulty wind turbine through active power dispatch under generator cooling system fault. The simulation results showed that the proposed strategy can reduce the temperature rise of the generator under fault conditions. The power loss compared with shut-down is much lower.

Similarly, for the stator ITSC fault of DFIG, Paper C used the fault model to calculate the power limitation with a known fault level. The simulation results showed that this method can prevent the faulty phase from further deterioration caused by the excessive winding temperature at the initial stage of the ITSC fault. For a common fault like ITSC, this method can protect the generator and prevent the faulty turbine from causing excessive downtime. In addition to the power limitation of the faulty wind turbine through power dispatch optimization, the ITSC fault ride-through strategy proposed by Paper D derated the faulty turbine through fault diagnosis and the PI control of generator torque and pitch angle at the turbine level. The simulation results showed that the proposed strategy can effectively reduce the faulty phase current to the rated current value and prevent the insulation aging caused by excessive fault current. And there is no need to estimate the fault level, which also avoids the negative effects caused by estimation errors.

To increase the power of the wind farm and reduce the power loss caused by the faulty wind turbine, the Min-C_{rmt} strategy proposed by Paper E can reduce the thrust coefficient of the upstream wind turbine as much as possible at the turbine level, thereby reducing the wind speed deficit of the downstream wind turbines caused by wake effects. The active power dispatch optimization based on the wake model and PSO algorithm in Paper B, C and F can improve the power of wind farms at the farm level.

Through the analysis of different down-regulation strategies, Paper F found that the Min-C_t strategy can increase the power of the wind farm, but for the wind turbines with ITSC fault, Max-ω strategy is more suitable because it derates less power than that in Min-C_t strategy. Therefore, the use of switching power down-regulation strategy of the faulty wind turbine can better avoid the excessive power loss of the faulty wind turbine and reduce the impact of the fault on the power of the wind farm.

The overall conclusion was that the use of derating strategy can effectively avoid the deterioration of some heat-related generator faults at the initial stage, such as generator cooling system faults and stator ITSC fault. The power limitations of these faults that can make the faulty wind turbine continue to operate safely can be obtained through the analysis of the fault models. Different down-regulation strategies have different effects on faults and wake effects. The reasonable selection of down-regulation strategies can reduce the power loss caused by the faulty wind turbine and increase the power of the wind farm. Active power dispatch optimization considering wake effects and fault conditions is also one of the means to improve the wind farm power. The combination of turbine level control and wind farm-level optimization can greatly improve the operating capability of wind farms under wind turbine fault conditions, reduce wind farm O&M costs, and improve wind power's competitiveness in the renewable energy market.

5.2 Future Work

In addition to research in this thesis, there are still many issues worthy of consideration and study regarding wind farm control under generator faults. Future work will focus on the followings:

- More fault modes suitable for derating strategies to reduce the impact of faults need to be studied. The ideas and methods proposed in this thesis are also applicable to these faults. But the fault model needs further in-depth research or verification in experiments. In this way, it can more safely reduce the power loss on the premise of protecting the faulty wind turbine.

- Since the PSO-based optimization is adopted in this thesis, the engineering models with low accuracy is used. However, some studies have proposed more wake models with higher accuracy. The use of the high fidelity model can get a more accurate estimation of the actual situation of the wake, and thus obtain more accurate results.

- At present, more and more researches have proved that the yaw-based wind farm power optimization has greater potential. And the development of LIDAR technology will further enhance the actual effect of this method. Therefore, in future research, yaw-based control or a combination of yaw-based control and axial induction-based control can be used as options for improving the power of wind farms.

- During the operation of a wind farm, in addition to power output, fatigue loads are also very worthy of attention. If loads of the key components of the wind turbine and the load distribution of the wind farm can be taken into account, it will be more conducive to the healthy operation of the wind farm. By adding the health level estimation of wind turbines to the wind farm control and optimization, the O&M costs can be further reduced, especially for offshore wind farms.

References

[1] (2016) What are the advantages and disadvantages of offshore wind farms? [Online]. Available: https://www.americangeosciences.org/critical-issues/faq/what-are-advantages-and-disadvantages-offshore-wind-farms

[2] (2020) Gwec: Over 60gw of wind energy capacity installed in 2019, the second-biggest year in history. [Online]. Available: https://gwec.net/gwec-over-60gw-of-wind-energy-capacity-installed-in-2019-the-second-biggest-year-in-history/

[3] (2020) World wind capacity at 650,8 gw, corona crisis will slow down markets in 2020, renewables to be core of economic stimulus programmes. [Online]. Available: https://wwindea.org/blog/2020/04/16/world-wind-capacity-at-650-gw/

[4] M. Abadi, S. Cruz, A. Gonçalves, A. Mendes, A. Ribeiro, and F. Silva, "Inter-turn fault detection in doubly-fed induction generators for wind turbine applications using the stator reactive power analysis," 2014.

[5] A. Abdel-Khalik, M. Masoud, S. Ahmed, and A. Massoud, "Calculation of derating factors based on steady-state unbalanced multiphase induction machine model under open phase (s) and optimal winding currents," *Electric power systems research*, vol. 106, pp. 214–225, 2014.

[6] L. Alberti and N. Bianchi, "A coupled thermal–electromagnetic analysis for a rapid and accurate prediction of im performance," *IEEE Transactions on Industrial Electronics*, vol. 55, no. 10, pp. 3575–3582, 2008.

[7] J. Annoni, P. M. Gebraad, A. K. Scholbrock, P. A. Fleming, and J.-W. v. Wingerden, "Analysis of axial-induction-based wind plant control using an engineering and a high-order wind plant model," *Wind Energy*, vol. 19, no. 6, pp. 1135–1150, 2016.

[8] M. Arkan, D. Kostic-Perovic, and P. Unsworth, "Modelling and simulation of induction motors with inter-turn faults for diagnostics," *Electric Power Systems Research*, vol. 75, no. 1, pp. 57–66, 2005.

[9] M. Bastankhah and F. Porté-Agel, "Wind farm power optimization via yaw angle control: A wind tunnel study," *Journal of Renewable and Sustainable Energy*, vol. 11, no. 2, p. 023301, 2019.

[10] R. L. Busby, *Wind power: The industry grows up*. PennWell Books, 2012.

[11] J. Carroll, A. McDonald, and D. McMillan, "Failure rate, repair time and unscheduled o&m cost analysis of offshore wind turbines," *Wind Energy*, vol. 19, no. 6, pp. 1107–1119, 2016.

[12] R. G. De Almeida, E. D. Castronuovo, and J. P. Lopes, "Optimum generation control in wind parks when carrying out system operator requests," *IEEE transactions on power systems*, vol. 21, no. 2, pp. 718–725, 2006.

[13] D. Dilip and F. Porté-Agel, "Wind turbine wake mitigation through blade pitch offset," *Energies*, vol. 10, no. 6, p. 757, 2017.

[14] H. Douglas, P. Pillay, and P. Barendse, "The detection of interturn stator faults in doubly-fed induction generators," in *Fourtieth IAS Annual Meeting. Conference Record of the 2005 Industry Applications Conference, 2005.*, vol. 2. IEEE, 2005, pp. 1097–1102.

[15] F. Ebrahimi, A. Khayatiyan, and E. Farjah, "A novel optimizing power control strategy for centralized wind farm control system," *Renewable energy*, vol. 86, pp. 399–408, 2016.

[16] J. Faiz and A. M. Takbash, "Derating of three-phase squirrel-cage induction motor under broken bars fault," *Facta Universitatis, Series: Automatic Control and Robotics*, vol. 12, no. 3, pp. 147–156, 2014.

[17] P. Fleming, P. M. Gebraad, S. Lee, J.-W. van Wingerden, K. Johnson, M. Churchfield, J. Michalakes, P. Spalart, and P. Moriarty, "Simulation comparison of wake mitigation control strategies for a two-turbine case," *Wind Energy*, vol. 18, no. 12, pp. 2135–2143, 2015.

[18] P. Fleming, J. King, K. Dykes, E. Simley, J. Roadman, A. Scholbrock, P. Murphy, J. K. Lundquist, P. Moriarty, K. Fleming *et al.*, "Initial results from a field campaign of wake steering applied at a commercial wind farm–part 1," *Wind Energy Science (Online)*, vol. 4, no. NREL/JA-5000-73991, 2019.

[19] P. Flores, A. Tapia, and G. Tapia, "Application of a control algorithm for wind speed prediction and active power generation," *Renewable Energy*, vol. 30, no. 4, pp. 523–536, 2005.

[20] P. M. Gebraad, F. Teeuwisse, J. Van Wingerden, P. A. Fleming, S. Ruben, J. Marden, and L. Pao, "Wind plant power optimization through yaw control using a parametric model for wake effects—a cfd simulation study," *Wind Energy*, vol. 19, no. 1, pp. 95–114, 2016.

[21] P. M. Gebraad, F. C. van Dam, and J.-W. van Wingerden, "A model-free distributed approach for wind plant control," in *2013 American Control Conference*. IEEE, 2013, pp. 628–633.

[22] T. Gocmen, P. Van der Laan, P.-E. Rethore, A. P. Diaz, G. C. Larsen, and S. Ott, "Wind turbine wake models developed at the technical university of denmark: A review," *Renewable and Sustainable Energy Reviews*, vol. 60, pp. 752–769, 2016.

[23] J. D. Grunnet, M. Soltani, T. Knudsen, M. Kragelund, and T. Bak, "Aeolus toolbox for dynamics wind farm model, simulation and control," in *The European Wind Energy Conference & Exhibition, EWEC*, vol. 2010, 2010.

[24] T. Horvat, V. Spudić, and M. Baotić, "Quasi-stationary optimal control for wind farm with closely spaced turbines," in *2012 Proceedings of the 35th International Convention MIPRO*. IEEE, 2012, pp. 829–834.

[25] M. F. Howland, S. K. Lele, and J. O. Dabiri, "Wind farm power optimization through wake steering," *Proceedings of the National Academy of Sciences*, vol. 116, no. 29, pp. 14 495–14 500, 2019.

[26] Z. Jinhua, L. Yongqian, D. Infield, M. Yuanchi, C. Qunshi, and T. De, "Optimal power dispatch within wind farm based on two approaches to wind turbine classification," *Renewable energy*, vol. 102, pp. 487–501, 2017.

[27] H. Jorgensen, M. Nielsen, R. Barthelmie, and N. Mortensen, “Modelling offshore wind resources and wind conditions,” 01 2005.

[28] S. Kanev and D. van de Hoek, “Reducing wind turbine loads with down-regulation,” ECN, Tech. Rep., 2017.

[29] W. Kersting and W. Phillips, “Phase frame analysis of the effects of voltage unbalance on induction machines,” *IEEE Transactions on Industry Applications*, vol. 33, no. 2, pp. 415–420, 1997.

[30] A. C. Kheirabadi and R. Nagamune, “A quantitative review of wind farm control with the objective of wind farm power maximization,” *Journal of Wind Engineering and Industrial Aerodynamics*, vol. 192, pp. 45–73, 2019.

[31] T. Knudsen, T. Bak, and M. Svenstrup, “Survey of wind farm control—power and fatigue optimization,” *Wind Energy*, vol. 18, no. 8, pp. 1333–1351, 2015.

[32] P. C. Krause, O. Wasynczuk, S. D. Sudhoff, and S. Pekarek, *Analysis of electric machinery and drive systems*. Wiley Online Library, 2002, vol. 2.

[33] J. Lee and F. Zhao, *GLOBAL WIND REPORT 2019*, 03 2020.

[34] Q. Li, Y. Su, and M. Tan, “Coordinative optimization on fatigue distribution and active power in wind farms,” in *2016 International Symposium on Electrical Engineering (ISEE)*. IEEE, 2016, pp. 1–6.

[35] Q. Lu, “Fault diagnosis and fault tolerant control of dfig based wind turbine system,” Ph.D. dissertation, University of Manchester, 2012.

[36] Q. Lu, T. Breikin, and H. Wang, “Modelling and fault diagnosis of stator inter-turn short circuit in doubly fed induction generators,” *IFAC Proceedings Volumes*, vol. 44, no. 1, pp. 1013–1018, 2011.

[37] J. R. Marden, S. D. Ruben, and L. Y. Pao, “A model-free approach to wind farm control using game theoretic methods,” *IEEE Transactions on Control Systems Technology*, vol. 21, no. 4, pp. 1207–1214, 2013.

[38] M. Mirzaei, T. Göçmen, G. Giebel, P. E. Sørensen, and N. K. Poulsen, “Turbine control strategies for wind farm power optimization,” in *2015 American Control Conference (ACC)*. IEEE, 2015, pp. 1709–1714.

[39] M. Mirzaei, M. Soltani, N. K. Poulsen, and H. H. Niemann, “Model based active power control of a wind turbine,” in *2014 American Control Conference*. IEEE, 2014, pp. 5037–5042.

[40] I. Ngamroo, “Review of dfig wind turbine impact on power system dynamic performances,” *IEEJ Transactions on electrical and electronic engineering*, vol. 12, no. 3, pp. 301–311, 2017.

[41] K. Nilsson, S. Ivanell, K. S. Hansen, R. Mikkelsen, J. N. Sørensen, S.-P. Breton, and D. Henningson, “Large-eddy simulations of the lillgrund wind farm,” *Wind Energy*, vol. 18, no. 3, pp. 449–467, 2015.

[42] S. Pfaffel, S. Faulstich, and K. Rohrig, “Performance and reliability of wind turbines: A review,” *energies*, vol. 10, no. 11, p. 1904, 2017.

[43] H. Polinder, J. A. Ferreira, B. B. Jensen, A. B. Abrahamsen, K. Atallah, and R. A. McMahon, “Trends in wind turbine generator systems,” *IEEE Journal of emerging and selected topics in power electronics*, vol. 1, no. 3, pp. 174–185, 2013.

[44] L. M. Popa, B.-B. Jensen, E. Ritchie, and I. Boldea, “Condition monitoring of wind generators,” in *38th IAS Annual Meeting on Conference Record of the Industry Applications Conference, 2003.*, vol. 3. IEEE, 2003, pp. 1839–1846.

[45] F. Porte-Agel, M. Bastankhah, and S. Shamsoddin, “Wind-turbine and wind-farm flows: a review,” *Boundary-Layer Meteorology*, vol. 174, no. 1, pp. 1–59, 2020.

[46] W. Qiao and D. Lu, “A survey on wind turbine condition monitoring and fault diagnosis—part i: Components and subsystems,” *IEEE Transactions on Industrial Electronics*, vol. 62, no. 10, pp. 6536–6545, 2015.

[47] Y. Qiu, W. Zhang, M. Cao, Y. Feng, and D. Infield, “An electro-thermal analysis of a variable-speed doubly-fed induction generator in a wind turbine,” *Energies*, vol. 8, no. 5, pp. 3386–3402, 2015.

[48] B. Rasmus, R. Knud, W. Anna-Kathrin, and L. Silke, “Capacity densities of european offshore wind farms,” *Deutsche Wind Guard GmbH, Germany*, 2018.

[49] M. D. Reder, E. Gonzalez, and J. J. Melero, “Wind turbine failures-tackling current problems in failure data analysis,” in *Journal of Physics: Conference Series*, vol. 753, no. 072027. IOP Publishing, 2016, pp. 1–11.

[50] J. Schepers and S. Van der Pijl, “Improved modelling of wake aerodynamics and assessment of new farm control strategies,” in *Journal of Physics: Conference Series*, vol. 75, no. 1, 2007, p. 012039.

[51] D. Shah, S. Nandi, and P. Neti, “Stator-interturn-fault detection of doubly fed induction generators using rotor-current and search-coil-voltage signature analysis,” *IEEE Transactions on Industry Applications*, vol. 45, no. 5, pp. 1831–1842, 2009.

[52] U. Shipurkar, K. Ma, H. Polinder, F. Blaabjerg, and J. A. Ferreira, “A review of failure mechanisms in wind turbine generator systems,” in *2015 17th European Conference on Power Electronics and Applications (EPE’15 ECCE-Europe)*. IEEE, 2015, pp. 1–10.

[53] C. Sourkounis and P. Tourou, “Grid code requirements for wind power integration in europe,” in *Conference Papers in Energy*, vol. 2013. Hindawi, 2013.

[54] M. Steinbuch, W. De Boer, O. Bosgra, S. Peeters, and J. Ploeg, “Optimal control of wind power plants,” *Journal of Wind Engineering and Industrial Aerodynamics*, vol. 27, no. 1-3, pp. 237–246, 1988.

[55] R. M. Tallam, T. G. Habetler, and R. G. Harley, “Transient model for induction machines with stator winding turn faults,” *IEEE Transactions on Industry Applications*, vol. 38, no. 3, pp. 632–637, 2002.

[56] B. Venkataraman, B. Godsey, W. Premerlani, E. Shulman, M. Thaku, and R. Midence, “Fundamentals of a motor thermal model and its applications in motor protection,” in *58th Annual Conference for Protective Relay Engineers, 2005.* IEEE, 2005, pp. 127–144.

[57] WindEurope, *Wind energy in Europe in 2019-Trends and statistics*, 02 2020.

[58] J.-h. Zhang, Y.-q. Liu, D. Tian, and J. Yan, “Optimal power dispatch in wind farm based on reduced blade damage and generator losses,” *Renewable and Sustainable Energy Reviews*, vol. 44, pp. 64–77, 2015.

Part II

Papers

Paper A

Active Power Dispatch Strategy of Wind Farms under Generator Faults

Kuichao Ma, Jiangsheng Zhu, Mohsen N. Soltani, Amin Hajizadeh, Peng Hou, Zhe Chen

The paper has been published in the
Proceedings of the European Safety and Reliability Conference 2018 : Safe Societies in a Changing World pp. 2147–2152, 2018.

Paper B

Optimal Power Dispatch of an Offshore Wind Farm under Generator Fault

Kuichao Ma, jiangsheng zhu, Mohsen N. Soltani, Amin Hajizadeh, Zhe Chen

The paper has been published in the
Applied Sciences Vol. 9(6), pp. 1184, 2019.

Paper C

Active Power Optimisation for Wind Farms under Generator Inter-Turn Short-Circuit Fault

Kuichao Ma, Mohsen N. Soltani, Amin Hajizadeh, jiangsheng Zhu, Zhe Chen

The paper has been published in the
IET Renewable Power Generation , 2020.

Paper D

Inter-Turn Short-Circuit Fault-Ride-Through for DFIG Wind Turbines

Kuichao Ma, jiangsheng Zhu, Mohsen N. Soltani, Amin Hajizadeh, Zhe Chen

The paper has been published in the
Ifac-papersonline, 2020 , 2020.

Paper E

Wind Turbine Down-Regulation Strategy for Minimum Wake Deficit

Kuichao Ma, Jiangsheng Zhu, Mohsen N. Soltani, Amin Hajizadeh, Zhe Chen

The paper has been published in the
Proceedings of 2017 11th Asian Control Conference (ASCC) pp. 2652–2656, 2017.

Paper F

Wind Farms Power Optimization and Fault Ride-Through under Inter-Turn Short-Circuit Fault

Kuichao Ma, Mohsen Soltani, Amin Hajizadeh, Jiangsheng Zhu, Zhe Chen

The manuscript has been submitted and under review for the *Energies*

ISSN (online): 2446-1636
ISBN (online): 978-87-7210-940-4

AALBORG UNIVERSITY PRESS